Seach for Two-Particle Muon Decay to Positron and Goldstone Massless Boson – Familon. Project of Experiment

PNPI (Gatchina) - V.A.Andreev, N.F.Bondarev, V.L.Golovtsov, V.A.Gordeev, Yu.V.Elkin, V.G.Ivochkin, E.M.Karasev, E.N. Komarov, C.V.Kosijanenko, A.G.Krivshich, M.P.Levchenko, Yu.A.Scheglov, G.V.Scherbakov, S.I.Vorobyov, A.A.Zhdanov

JINR (Dubna) - V.G.Grebinnik, K.I.Gritsaj, S.A.Gustov, V.N.Duginov, V.A.Zhukov, T.N.Mamedov, I.V.Mirokhin, V.G.Olshevsky, A.V.Stoykov

ITEP (Moscow) – K.E.Gusev, V.S.Demidov, E.V.Demidova N.A.Khaldeeva, G.I.Saveliev, A.Yu.Sokolov, Yu.P.Shkurenko

IPM (Moscow) – M.Yu.Khlopov

PROJECT SPOKESMAN V.A.GORDEEV

COORDINATOR FROM JINR V.N.DUGINOV


Электросила
им. С.М.Кирова

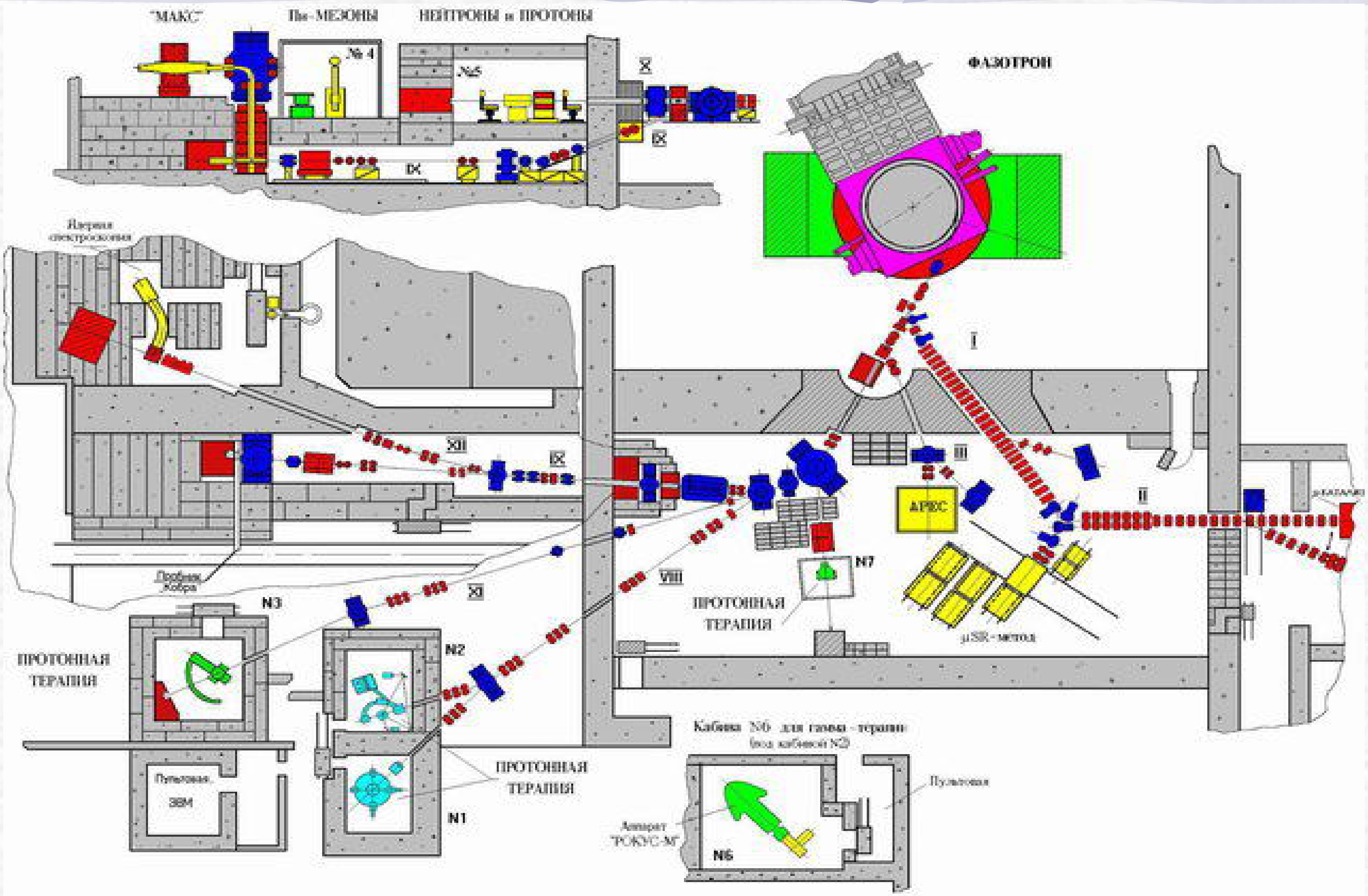

СХЕМА ПУЧКОВ ФАЗОТРОНА ЛЯП ОИЯИ

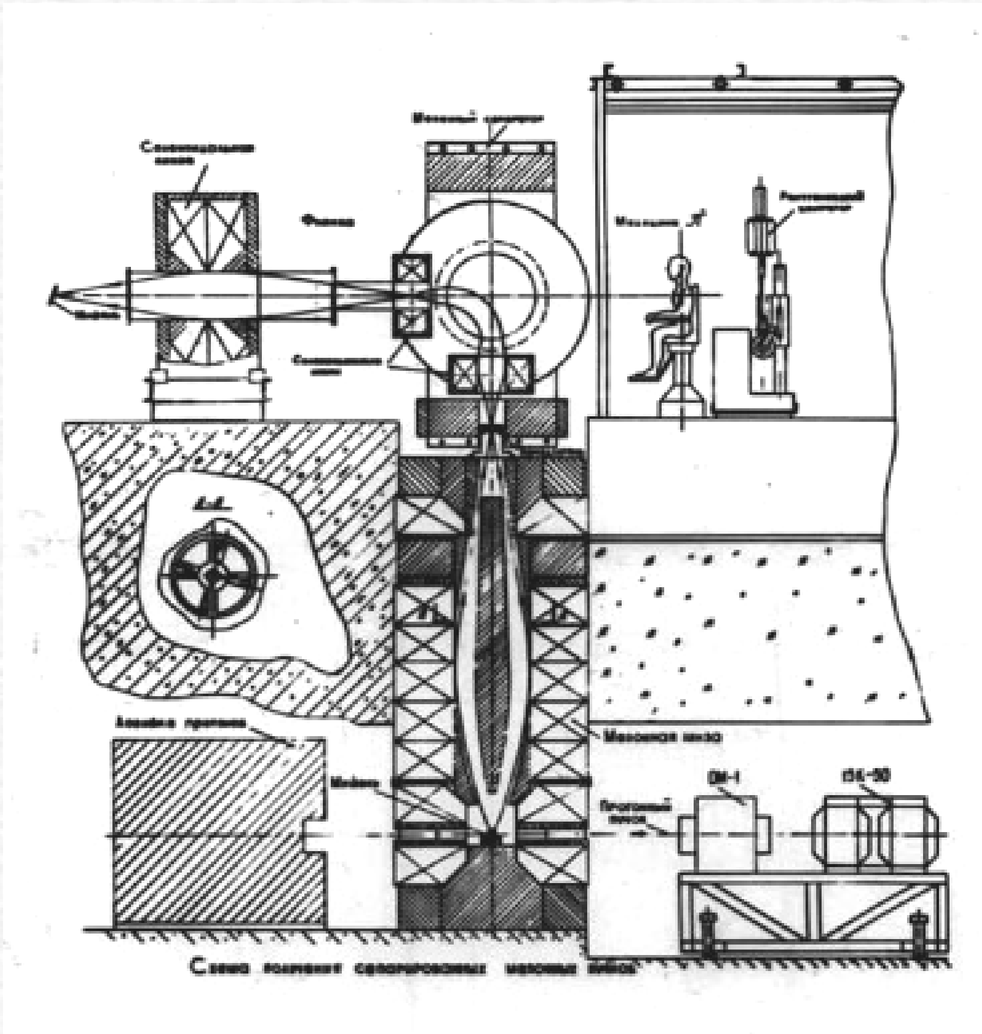

Intensity of charged particles

Intensity of charged particles from channel IX of Dubna phasotron per 1 μA of the proton beam. W–target. Momentum spred is $\Delta p/p \simeq 5.8\%$

Particle momentum MeV/c	Intensity on area of 80 cm^2, $10^5\ 1/s$					
	Positively charged			Negatively charged		
	e^+	μ^+	π^+	e^-	μ^-	π^-
76	32	2.6	13			
95	24	3.6	30	18	1.4	10
112	16	3.8	46	11	1.2	15
123	8.0	2.9	50	8.0	0.9	17
149	4.3	1.2	42	5.0	$\leq$0.7	18
165	2.8	0.6	35	3.8	$\leq$0.6	17

Flux density and intensity of surface μ^+– mesons from channel IX of Dubna phasotron per 1 μA of the proton beam. Cu–target. $\Delta p/p \simeq 5.8\%$

Momentum MeV/c	$N_{\mu^+}/N_{e^+}\%$	Flux density $\times 10^3\ 1/cm^2 \cdot s \cdot \mu A$	Intensity on area of 80 cm^2, $\times 10^5\ 1/s \cdot \mu$ A
26	1.9	3.8	3.0
28	3.3	6.6	5.3
30	2.7	5.4	4.3
32	0.2	0.4	

For separated beam of 24 MeV/c surface mesons the intensity $\simeq 2 \cdot 10^5 1/s \cdot \mu A$ was attaind with the ratio $N_{\mu^+}/N_{e^+} \approx 1$

Таблица 1

Распад мюона		$m_{\mu^\pm} = 105{,}6583568(52)$ МэВ	$\tau_{\mu^\pm} = 2{,}19703(4) \times 10^{-6}$ сек	
Моды распада μ^-		Отношение (Γ_j/Γ)	Уровень достов.	
$e^-\bar{\nu}_e\nu_\mu$		$\approx 100\%$		
$e^-\bar{\nu}_e\nu_\mu\gamma$		$(1{,}4 \pm 0{,}4)\%$		
$e^-\bar{\nu}_e\nu_\mu e^+e^-$		$(3{,}4 \pm 0{,}4) \times 10^{-5}$		
Моды распада с несохранением LF (Lepton Family) числа				
$e^-\nu_e\bar{\nu}_\mu$	LF	$< 1{,}2\%$	90%	
$e^-\gamma$	LF	$< 1{,}2 \times 10^{-11}$	90%	
$e^-e^+e^-$	LF	$< 1{,}0 \times 10^{-12}$	90%	
$e^-2\gamma$	LF	$< 7{,}2 \times 10^{-11}$	90%	
$\mu^-Ti \to e^-Ti$	LF	$< 4{,}3 \times 10^{-12}$	90%	
$\mu^-Ti \to e^+Ca$	LF	$< 3{,}6 \times 10^{-11}$	90%	
$\mu^+e^- \to \mu^-e^+$	LF	$\leq 4{,}7 \times 10^{-7}$	90%	**
$\mu^+e^- \to \mu^-e^+$	LF	$< 8{,}3 \times 10^{-11}$	90%	***

* Моды распада μ^+ зарядовосопряженны приведенным выше

** результат эксперимента группы ПИЯФ–ОИЯИ, 1997

*** результат PSI в магнитном поле 0.1 Тс, 1999

Таблица 2

Распад пиона		$m_{\pi^\pm} = 139{,}57018(35)$ МэВ	$\tau_{\pi^\pm} = 2{,}6033(5) \times 10^{-8}$ сек	
Моды распада π^+		Отношение (Γ_j/Γ)	Уровень достов.	
$\mu^+\nu_\mu$		$99{,}98770(4)\%$		
$e^+\nu_e$		$1{,}230(4) \times 10^{-4}$		
$\mu^+\nu_\mu\gamma$		$2{,}00(25) \times 10^{-4}$		
$e^+\nu_e\gamma$		$1{,}61(23) \times 10^{-7}$		
$e^+\nu_e\pi^\circ$		$1{,}025(34) \times 10^{-8}$		
$e^+\nu_e e^+e^-$		$3{,}2(5) \times 10^{-9}$		
$e^+\nu_e\nu\bar{\nu}$		$< 5 \times 10^{-6}$	90%	
Моды распада с несохр. L (Lepton) или LF (Lepton Family)				
$\mu^+\nu_e$	L	$< 1{,}5 \times 10^{-3}$	90%	
$\mu^+\nu_e$	LF	$< 8{,}0 \times 10^{-3}$	90%	
$\mu^-e^+e^+\nu$	LF	$< 1{,}6 \times 10^{-6}$	90%	**

* Моды распада π^- зарядовосопряжены приведенным выше

** результат эксперимента группы ОИЯИ, 1991

Higgs Bosons – H^0 and $H^{\pm\pm}$

Higgs Bosons — H^0 and $H^{\pm}$, Searches for

MASS LIMITS for $H^{\pm\pm}$ (doubly-charged Higgs boson)

VALUE (GeV)	CL%	DOCUMENT ID		TECN	COMMENT
>45.6	95	[142] ACTON	92M	OPAL	
• • • We do not use the following data for averages, fits, limits, etc. • • •					
		[143] GORDEEV	97	SPEC	muonium conversion
		[144] ASAKA	95	THEO	
>30.4	95	[145] ACTON	92M	OPAL	$T_3(H^{++}) = +1$
>25.5	95	[145] ACTON	92M	OPAL	$T_3(H^{++}) = 0$
none 6.5–36.6	95	[146] SWARTZ	90	MRK2	$T_3(H^{++}) = +1$
none 7.3–34.3	95	[146] SWARTZ	9´	MRK2	$T_3(H^{++}) = 0$

[142] ACTON 92M limit assumes $H^{\pm\pm} \rightarrow \ell^{\pm}\ell^{\pm}$ or $H^{\pm\pm}$ does not decay in the detector. Thus the regio.. $g_{\ell\ell} \approx 10^{-7}$ is not excluded.

[143] GORDEEV 97 s..arch for muonium-antimuonium conversion and find $G_{M\overline{M}}/G_F < 0.14$ (90% CL), where $G_{M\overline{M}}$ is the lepton-flavor violating effective four-fermion coupling. This limit may be onverted to $m_{H^{++}} > 210$ G V if the Yukawa copulings of H^{++} to ee and $\mu\mu$ are as large as the weak gauge coupling. For similar limits on muonium-antimuonium conversion, see the muon Particle Listings.

[144] ASAKA 95 point out that H^{++} decays dominantly to four fermions in a large region of parameter space where the limit of ACTON 9.M from the s arch of dilepton mode does not apply.

[145] ACTON 92M from $\Delta\Gamma_Z$ <40 MeV.

[146] SWARTZ 90 assume $H^{\pm\pm} \rightarrow \ell^{\pm}\ell^{\pm}$ (any flav·r). The limits are valid for the Higgs-lepton coupling $g(H\ell\ell) \gtrsim 7.4 \times 10^{-7}/[m_H/\text{GeV}]^{1/2}$. The limits improve somewhat for ee and $\mu\mu$ decay modes.

H^0 and $H^{\pm}$ REFERENCES

GORDEEV	97	PAN 60 1164	V.A. Gorde .+	(PNPI)
		Translated from YAF 60 1291.		
ASAKA	9.	PL B345 36	+Hikasa	(TOHOK)
ACTON	92M	PL B295 347	+Alexander, Allison, Allport, An lerson+	(OPAL Coll b.)
SWARTZ	90	PRL 64 2877	+Abrams, Adolphsen, Averill, Ballam+	(Mark II Collab.)

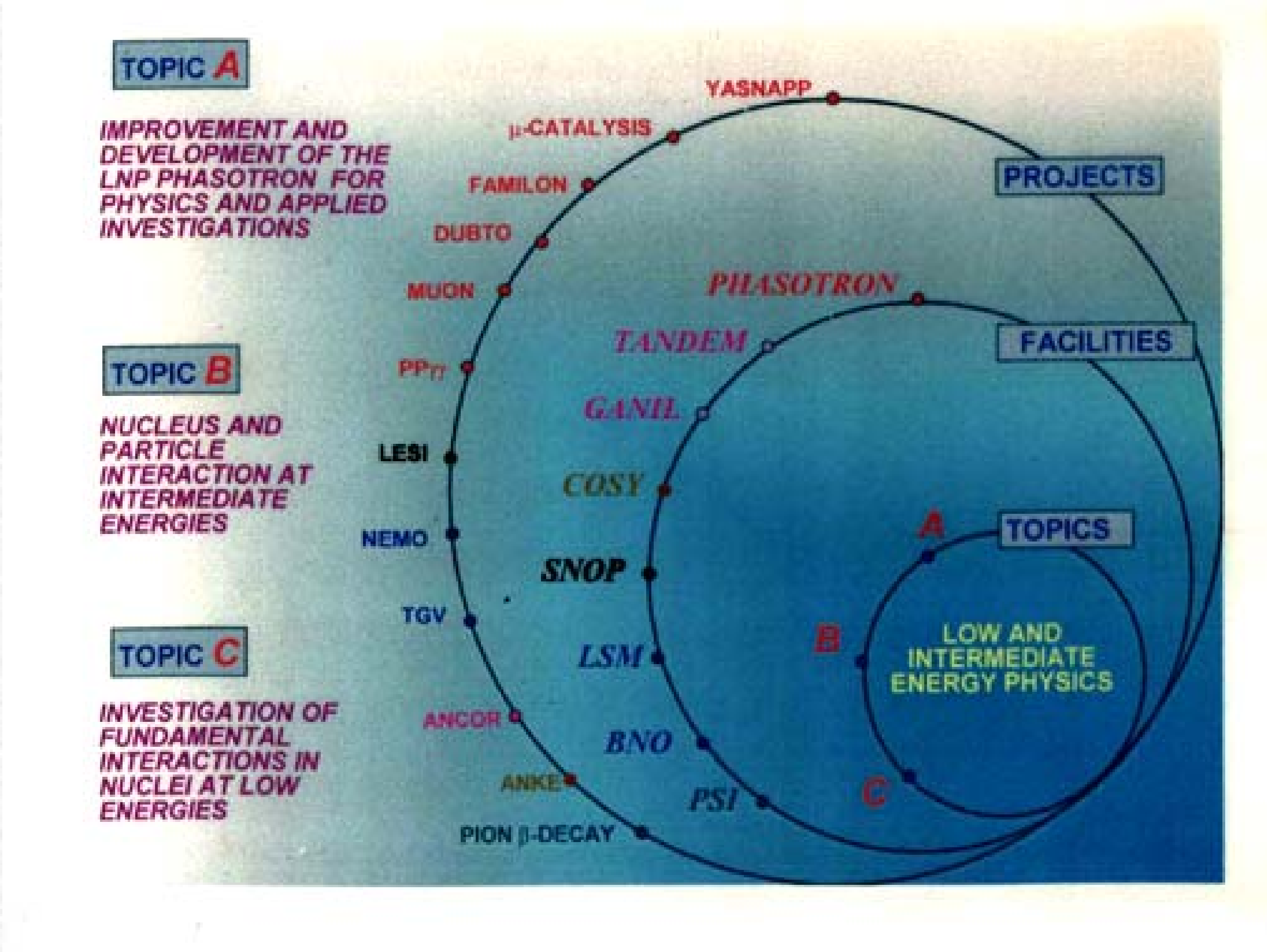
TOPIC A
IMPROVEMENT AND DEVELOPMENT OF THE LNP PHASOTRON FOR PHYSICS AND APPLIED INVESTIGATIONS
TOPIC B
NUCLEUS AND PARTICLE INTERACTION AT INTERMEDIATE ENERGIES
TOPIC C
INVESTIGATION OF FUNDAMENTAL INTERACTIONS IN NUCLEI AT LOW ENERGIES
YASNAPP
μ-CATALYSIS
FAMILON
DUBTO
MUON
PPγγ
LESI
NEMO
TGV
ANCOR
ANKE
PION β-DECAY
PROJECTS
PHASOTRON
TANDEM
GANIL
COSY
SNOP
LSM
BNO
PSI
FACILITIES
A
B
C
TOPICS
LOW AND INTERMEDIATE ENERGY PHYSICS

Dzhelepov Laboratory of Nuclear Problems

Investigations at Phasotron

(users' request facility)

Fundamental Investigations:

•DUBTO - Resonant behaviour of the both the $pp\pi^-$ and $nn\pi^+$ systems, produced in π^4He interaction.

•MUON – Investigation of the muon properties and the muon interactions with matter.

•FAMILON - The study of the two-particle muon decay on an electron and golston's massless boson.

•μ-CATALISIS- Measurements of muon cataslazed fusion cycling rate temperature dependence in a binary mixture D/T in the temperature range 40-300 K.

Applied investigations:

Cancer therapy;

SAD- Energy Amplifier

Machine development:

Upgrade of the Phasotron and its beam channels;

Design of external injection in the Phasotron.

OPERATION OF PHASOTRON (hours) 03.02-29.04.2003

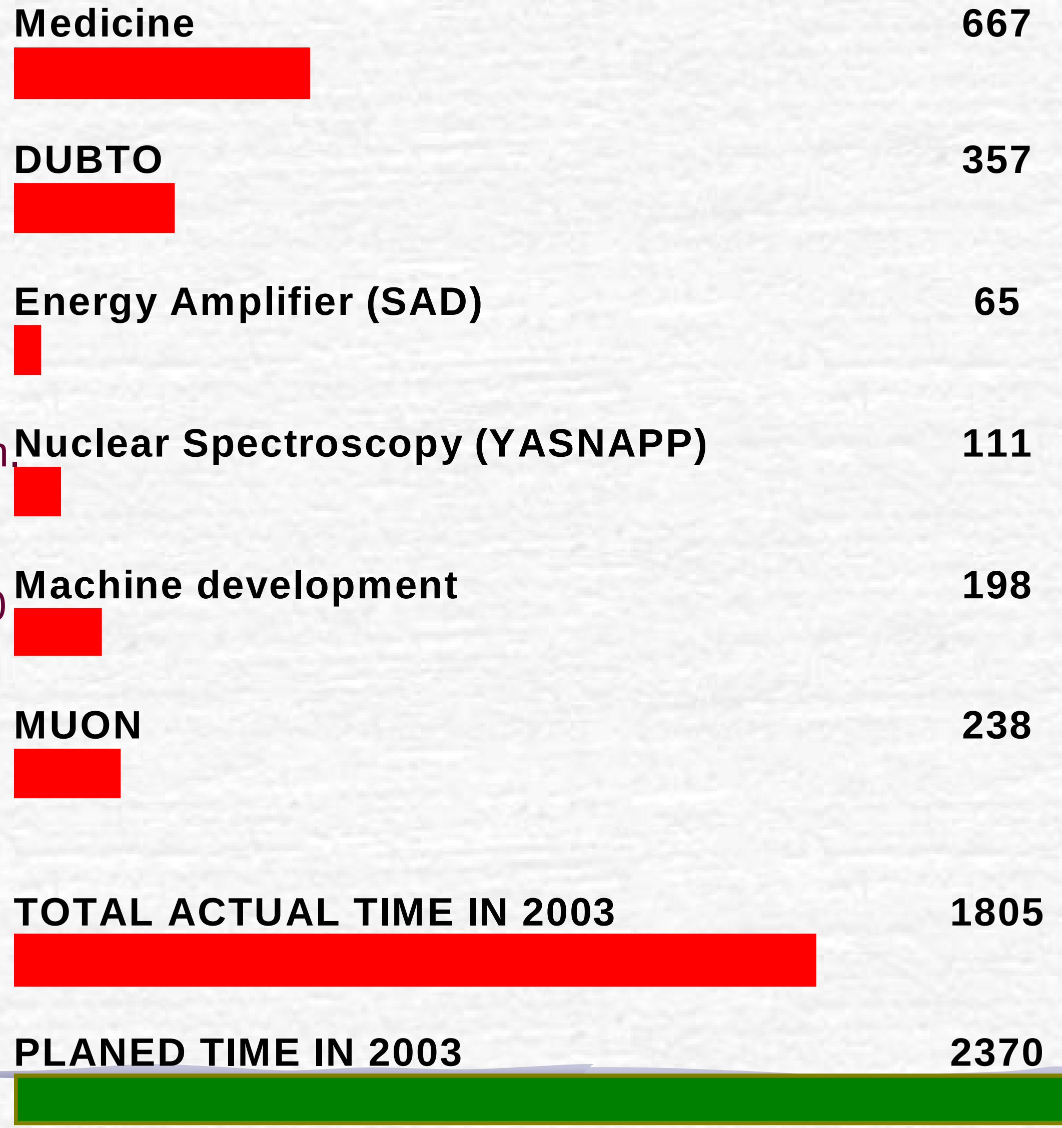

PROJECT 02-0987-92/2000

The Search for Two-particle Muon Decay to Electron and Goldstone Massless Boson (Familon)

SPOKESMAN VIKTOR GORDEEV
SPOKESMAN FROM JINR VIKTOR DUGINOV

PNPI(Gatchina)

JINR(Dubna)

RUSSIAN RESEARCH CENTRE "KURCHATOV INSTITUTE" РОССИЙСКИЙ НАУЧНЫЙ ЦЕНТР "КУРЧАТОВСКИЙ ИНСТИТУТ"

ITEP (Moscow)

$\mu \to e + \alpha$

$\mu \to e + \alpha$

F. Wilczek, Phys. Rev., v. 49, 1549 (1982)
G. Gelmini et al., Nucl Phys., v. B219, 31 (1983)
А.А. Ансельм, ЖЭТФ, т. 84, 1961 (1983)

$s \to d + \alpha, \quad \mu \to e + \alpha, \quad \nu_H \to \nu_L + \alpha$

В рамках реалистической $SU(5)xSU(3)_H$ модели взаимодей-ствие фамилона с кварками и лептонами описывается лагранжианом

$$L = \frac{\sqrt{2 m_\alpha m_s}}{<B>} \alpha (\bar{d} s + \bar{s} d) + \frac{\sqrt{2 m_e m_\mu}}{<B>} \alpha (\bar{\mu} e - \bar{e} \mu)$$

<B> - среднее вакуумное значение хигсовских полей

$$\Gamma_0(\mu \to e\alpha) = \frac{m_\mu^2 \quad m_e}{16\pi B_e^2}.$$ Оценка B_e=2 10^8 GeV $\quad$ T_0=4 сек$^{-1}$

$$B = \frac{\Gamma(\mu - e\alpha)}{\int_{E_{max}-\Delta E}^{E_{max}} \frac{d\Gamma(\mu - e\nu\bar{\nu})}{dE} dE} = \frac{6\pi^2 m_e}{B_e^2 G_F^2 m_\mu^3 \Delta\varepsilon},$$

$$\Delta\varepsilon = \frac{\Delta E}{E}.$$

→ Если B_e = 2 10^8, $\Delta\varepsilon=10^{-4}$ имеем B=4,5 %

Familon could serve as an axion in solving the strong CP puzzle.

Familon is also desirable in cosmology: the large-scale structure of the Universe could be naturally explained by the neutrino mass ~ (40 – 100) eV if such a “heavy” neutrino ν_H decays rather rapidly (10^8 – 10^9 years) to the “light” neutrino ν_L ($m(\nu_L) < 10$ eV) and the familon.

The most stringent constraint for the couplings of the familon is imposed by the absence of $K^+ \to \pi^+ + \alpha$ decay. This decay, however, occurs only due to scalar interaction of familon: for pseudoscalar coupling the matrix element $<\pi | \underline{s}\ i\gamma_5 d | K>$ vanishes by parity. But nondiagonal in flavour couplings of pseudogoldstone bosons can well be both scalar and pseudoscalar ones. For this reason the search for the $\mu \to e + \alpha$ decay appears to be important for the familon hypothesis, since scalar and pseudoscalar couplings contribute equally in this case.

The interaction of familon with massive neutrino leads to decay

$\nu_H \to \nu_L + \alpha$ with

$$\boldsymbol{\tau(\nu_H) = (16\,\pi\eta_\nu{}^2)/[m(\nu_H)^2 m(\nu_L)]}$$

If $\tau(\nu_H) \approx 5.10^8$ years, $m(\nu_H) \approx 100$ eV and $m(\nu_L) \approx 10$ eV

It requires $\eta_\nu \approx 2.10^8$ GeV.

Note that the absence of $K+ \to \pi+ + \alpha$ decay implies

$\eta_{sd} > 8.10^9$ GeV for the scalar coupling of familon.

Physical motivation

Welczek (1982), Anselm and Uraltsev (1983), Gelmini et al. (1983) have indicated to the possible existing of the massless goldston's bosons which changed fermion quantum numbers. The differential velocity $\mu \to e\ \alpha$ - decay is given by expression:

$$d\Gamma(\mu \to e\alpha) = \Gamma_0(\mu \to e\alpha)\left[1 - \vec{P}_\mu \vec{P}_e + 2(\vec{P}_e \cdot \vec{n})(\vec{P}_\mu \cdot \vec{n})\right]\frac{\sin\vartheta \cdot d\vartheta}{4},$$

where $\Gamma_0(\mu \to e\ \alpha)$ - full breadth of $\mu \to e\ \alpha$ - decay for a unpolarized muon, $\vec{P}_\mu$ & $\vec{P}_e$ - polarization μ and e , $\vec{n}$ - momentum direction of the positron.

The relative probability of the decay $\mu \to e\ \alpha$ to usual decay $\mu \to e\ \nu\bar{\nu}$ is determined by the ratio:

$$R_\alpha = \frac{\int_0^\pi d\Gamma(\mu \to e\alpha)}{\int_0^1 \int_0^\pi d\Gamma(\mu \to e\bar{\nu}\nu)} = \frac{\Gamma_0(\mu \to e\alpha)}{\Gamma_0(\mu \to e\bar{\nu}\nu)}.$$

The relative contribution of decay $\mu \to e\ \alpha$ to usual decay in the narrow power interval $\Delta\varepsilon$ on the spectrum edge:

$$B_\alpha = \frac{\int_0^\pi d\Gamma(\mu \to e\alpha)}{\int_{1-\Delta\varepsilon}^1 \int_0^\pi d\Gamma(\mu \to e\bar{\nu}\nu)}$$

As it is clear for the decay of the $\mu \to e\alpha$ in the extremity of the decay spectrum positrons $\mu^+ \to e^+ \nu\bar{\nu}$ the narrow peak should be observed.

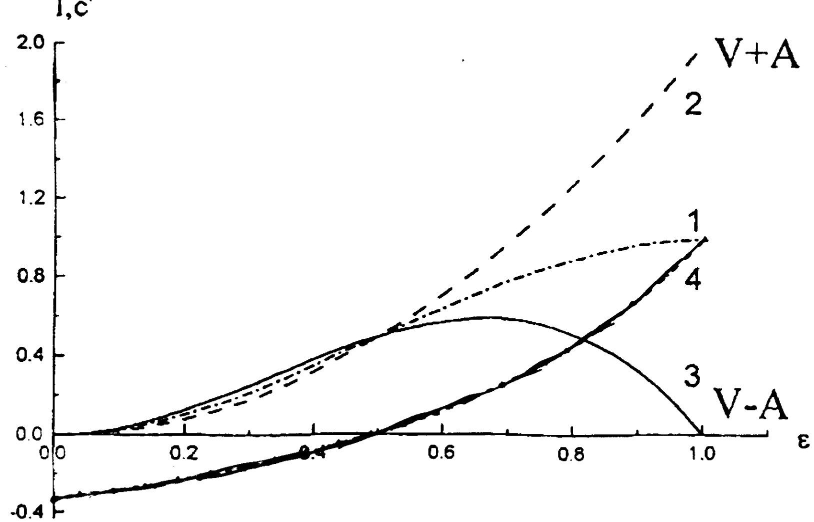

Fig.2. The energy dependence of the positron spectrum for $\mu \to e\, \nu\bar{\nu}$: decay (in relative units).
1 - continuous spectrum, 2,3 - for cos ϑ=-1,
4 - the asymmetry coefficient of $\mu \to e$ decay.

The neutrino-less mode of the muon decay will change this energy dependence of the asymmetry coefficient in high-energy region.

Table 1. Relative contribution $\mu \to e\, \alpha$ decay to the conventional decay in the energy interval **Δε.**

Δε	**10^{-3}**	**$5 \cdot 10^{-4}$**	**10^{-4}**	**$5 \cdot 10^{-5}$**	**10^{-5}**
B_α	$4{,}4\ 10^{-3}$	$8{,}8\ 10^{-3}$	$4{,}4\ 10^{-2}$	$8{,}8\ 10^{-2}$	0,435

Taking into account the finite capture angle and the detection energy range Δε, we have the following numbers of high energy positrons emitted along N^+ and opposite N^- to the muon spin direction of the decay $\mu \to e\, \nu\bar{\nu}$:

$$N^{\pm} = \int_{1-\Delta\varepsilon}^{1} \int_{0}^{\vartheta} \Gamma_0(\mu \to e\bar{\nu}\nu)[(3-2e) \pm (1-2\varepsilon)P_\mu \cos\vartheta] \cdot \varepsilon^2 d\varepsilon \cdot \sin\vartheta \, d\vartheta$$

Hence the asymmetry factor of high energy decay positrons $\mu \to e \, \nu\bar{\nu}$ will be

$$C' = \frac{N^+ - N^-}{N^+ + N^-} = \frac{P_\mu}{2}(1-2\Delta\varepsilon)(1+\cos\vartheta),$$

For the decay $\mu \to e \, \alpha$ we have due to the same reasons

$$N^+ = N^- = \tfrac{1}{2} \cdot \Gamma_0(\mu \to e\alpha)(1-\cos\vartheta),$$

and due to such process, the observed asymmetry factor of the $\mu \to e$ -decay is:

$$C'' = C' \frac{1}{1 + R_\alpha / (2\Delta\varepsilon)},$$

where C' and R_α were defined above. One can see that the ratio C''/C' is independent of ϑ. This fact is important for experimental statistic accumulation, because one can use wide-aperture detectors. In the Table 2 we have the values of $N^{\pm}$, C' and C'' for several different $\Delta\varepsilon$, ϑ, and $R=8\ 10^{-6}$.

From these considerations follows, that the experimental search for the decay $\mu \to e \, \alpha$ can be performed by using the standard μSR-equipment plus magnet spectrometer. The aim is to obtain the precession μSR-spectra of polarized muon stopped in matter with high density of conductivity electrons, in perpendicular magnetic field.

The presence of the decay $\mu \to e^+\alpha$ leads to lower asymmetry factor in the high energy region of positron spectra. The experiment has to be performed in the beam of low energy muons, generated in decays of π^+ -mesons, stopped in the surface layer of meson-producing target (the "surface" muons).

First such of type experiment was performed by A. Jodidio et al. in TRIUMF (Tr. 8-12)

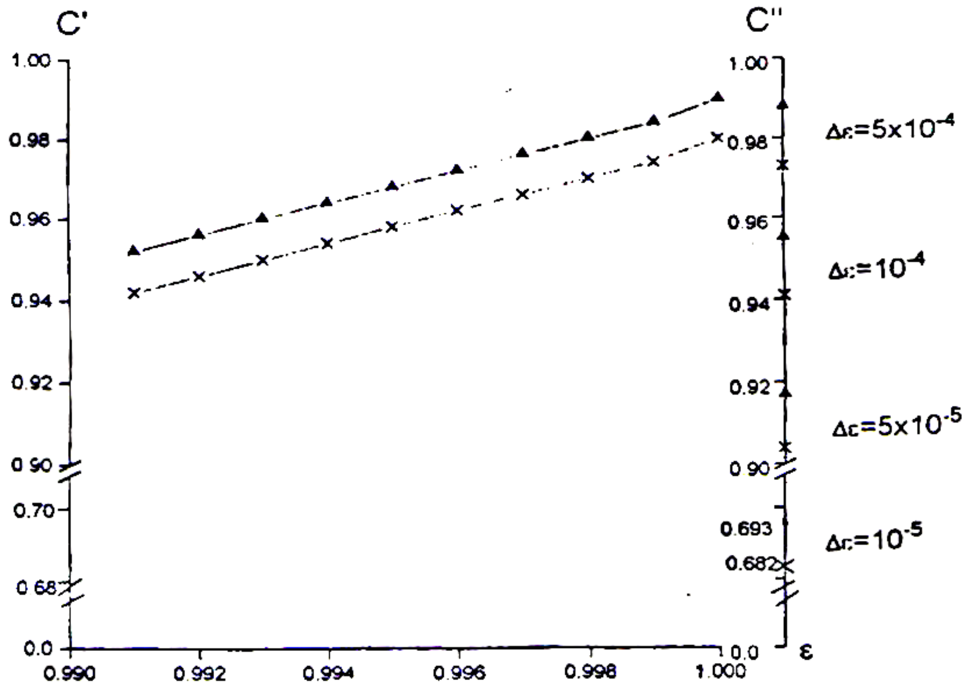

This Fig.3 illustrate the energy dependence of the asymmetry coefficient C' of the $\mu \rightarrow e\ \nu\bar{\nu}$-decay for two of angular capture. Δ- $\vartheta=5^0$ and × - $\vartheta=15^0$ and the asymmetry coefficient C'' in the spectrum end of the decay positrons for energy Δε.

It should be pointed out that the energy dependence of the asymmetry coefficient of positrons in the muon decay will be measured in the energy interval from 0,95 to 1.0 (in relative unites) with the step of 0.002. At the same time 25 μSR-spectra will be collected. The effect of the positron multiple scattering will cause a minor drop of the asymmetry coefficient measured. However, there is no physical reason to expect contribution of the positron multiple scattering to the energy dependence of asymmetry coefficient, which will be equivalent to the expected effect in a case of neutrino-less decay of muon.

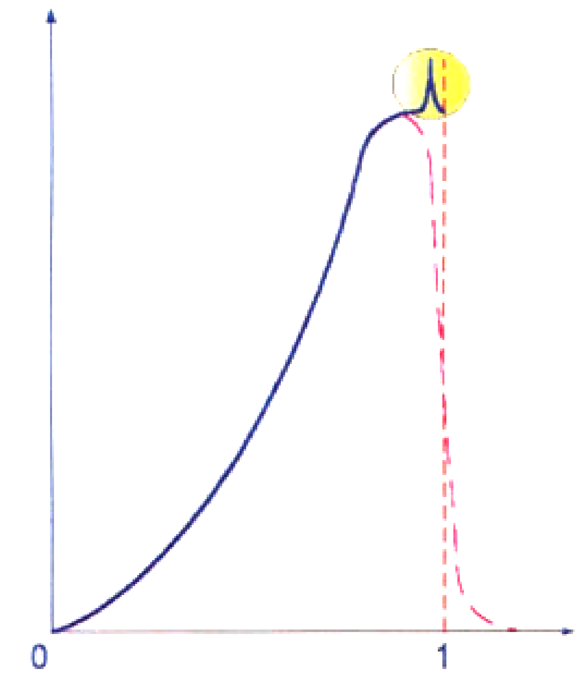
0
1

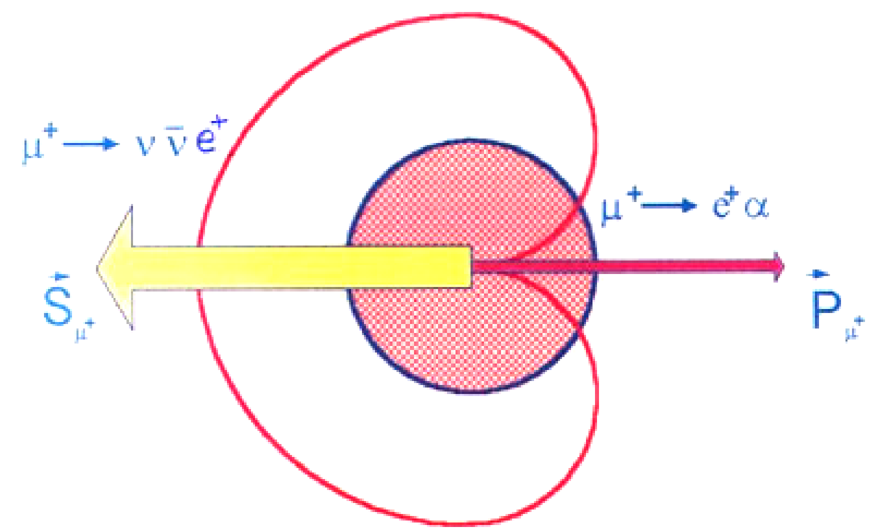
μ⁺ → ν ν̄ e⁺
μ⁺ → e⁺α
S_μ⁺
P_μ⁺

Searches for Goldstone Bosons (X^0)

Searches for Goldstone Bosons (X^0)

(Including Horizontal Bosons and Majorons.) Limits are for branching ratios.

VALUE	CL%	EVTS	DOCUMENT ID		TECN	COMMENT
• • • We do not use the following data for averages, fits, limits, etc. • • •						
			[134] DIAZ	98	THEO	$H^0 \rightarrow X^0 X^0$, $A^0 \rightarrow X^0 X^0 X^0$, Majoron
			[135] BOBRAKOV	91		Electron quasi-magnetic interaction
$<3.3 \times 10^{-2}$	95		[136] ALBRECHT	90E	ARG	$\tau \rightarrow \mu X^0$. Familon
$<1.8 \times 10^{-2}$	95		[136] ALBRECHT	90E	ARG	$\tau \rightarrow e X^0$. Familon
$<6.4 \times 10^{-9}$	90		[137] ATIYA	90	B787	$K^+ \rightarrow \pi^+ X^0$. Familon
$<1.1 \times 10^{-9}$	90		[138] BOLTON	88	CBOX	$\mu^+ \rightarrow e^+ \gamma X^0$. Familon
			[139] CHANDA	88	ASTR	Sun, Majoron
			[140] CHOI	88	ASTR	Majoron, SN 1987A
$<5 \times 10^{-6}$	90		[141] PICCIOTTO	88	CNTR	$\pi \rightarrow e \nu X^0$, Majoron
$<1.3 \times 10^{-9}$	90		[142] GOLDMAN	87	CNTR	$\mu \rightarrow e \gamma X^0$. Familon
$<3 \times 10^{-4}$	90		[143] BRYMAN	86B	RVUE	$\mu \rightarrow e X^0$. Familon
$<1. \times 10^{-10}$	90	0	[144] EICHLER	86	SPEC	$\mu^+ \rightarrow e^+ X^0$. Familon
$<2.6 \times 10^{-6}$	90		[145] JODIDIO	86	SPEC	$\mu^+ \rightarrow e^+ X^0$. Familon
			[146] BALTRUSAIT...	85	MRK3	$\tau \rightarrow \ell X^0$. Familon
			[147] DICUS	83	COSM	$\nu(\text{hvy}) \rightarrow \nu(\text{light}) X^0$

Search for right-handed currents in muon decay

Search for right-handed currents in muon decay

A. Jodidio,* B. Balke, J. Carr,† G. Gidal, K. A. Shinsky,‡ H. M. Steiner,
D. P. Stoker,§ M. Strovink, and R. D. Tripp
Lawrence Berkeley Laboratory and Department of Physics, University of California, Berkeley, California 94720

B. Gobbi
Department of Physics, Northwestern University, Evanston, Illinois 60201

C. J. Oram
TRIUMF, Vancouver, British Columbia V6T 2A3, Canc
(Received 27 May 1986)

Limits are reported on charged right-handed currents, based on precise n
point e^+ spectrum in μ^+ decay. Highly polarized μ^+ from a TRIUMF "su
stopped in pure metal foil and liquid-He targets selected to minimize depol
stopping target region either a spin-precessing transverse field (70 or 110 G)
tudinal field (0.3 or 1.1 T) was applied. Data collected with the spin-preces
the momentum calibration of the spectrometer. The spin-held data were u
tive e^+ rate at the momentum end point in a direction opposite to the μ^+ spi
dard muon-decay parameters this rate is given by $(1-\xi P_\mu \delta/\rho)$ where P_μ is
The combined 90% confidence lower limit from the analysis presented in th
analysis of the spin-precessed data by means of the muon-spin-rotati
$\xi P_\mu \delta/\rho > 0.9975$. For models with manifest left-right symmetry and massl
implies the 90% confidence limits $m(W_2) > 432$ GeV/c^2 and $-0.050 < \zeta <$
predominantly right-handed boson and ζ is the left-right mixing angle. Lin
the $\nu_{\mu L}$ mass and helicity in π^+ decay, non-$(V-A)$ couplings in helicity pr
scale of composite leptons, and the branching ratio for $\mu \to e + f$ where f
massless Nambu-Goldstone boson associated with flavor-symmetry breaking

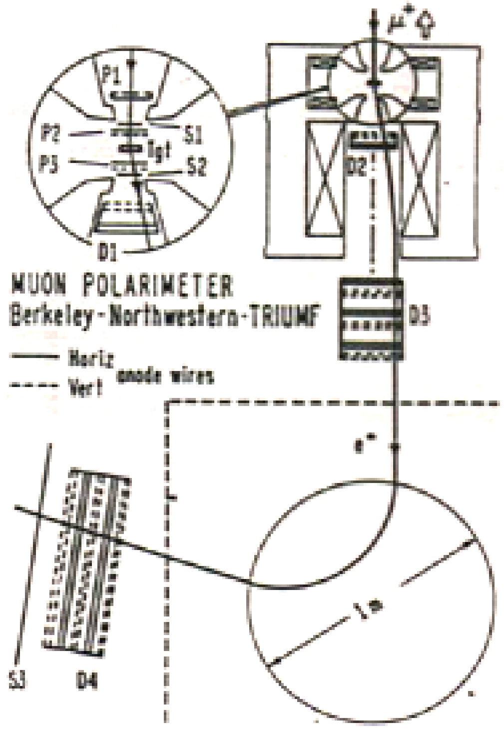

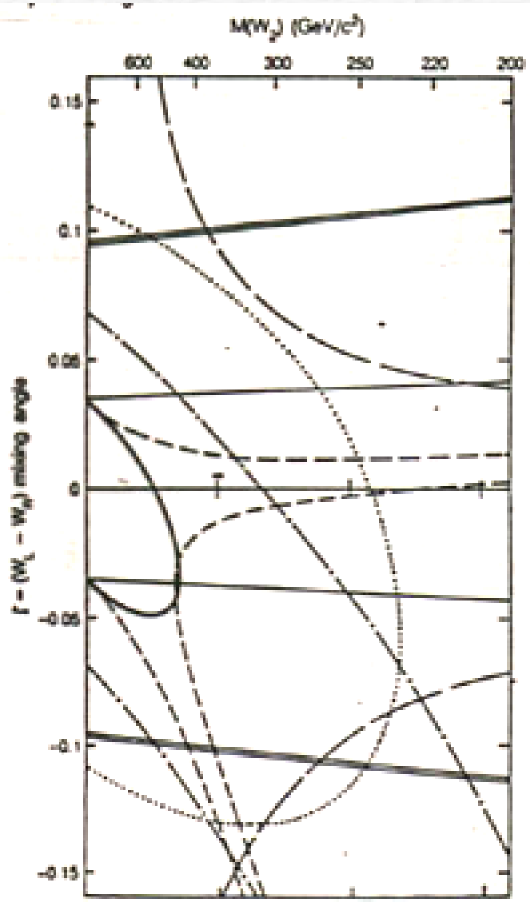

$P(e^+)/p(e^+)_{max}$

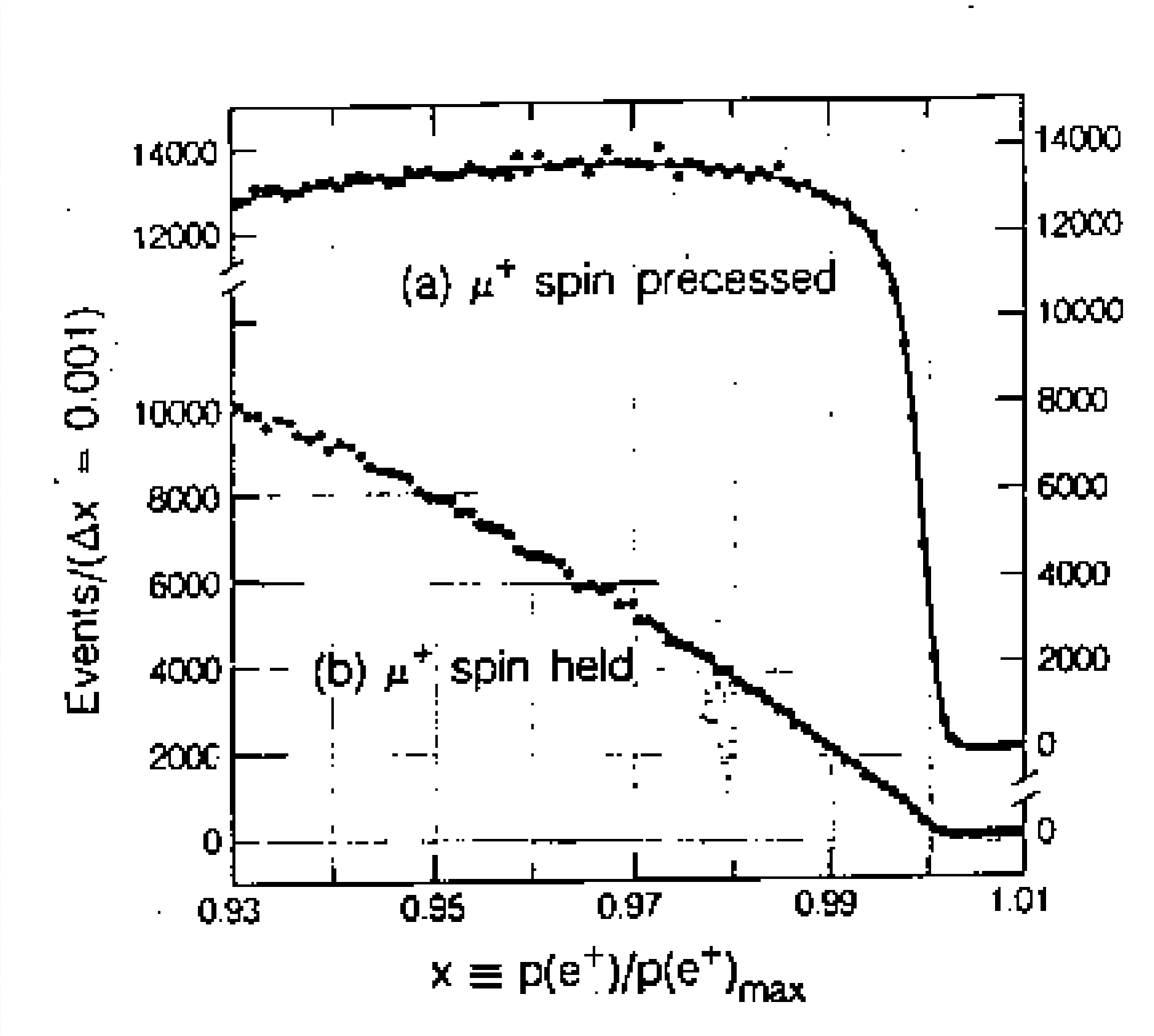

Events/(Δx = 0.001)
14000
12000
10000
8000
6000
4000
2000
0
(a) μ+ spin precessed
(b) μ+ spin held
0.93
0.95
0.97
0.99
1.01
x ≡ p(e+)/p(e+)max

TRIUMF limit on familon

- The decay rate $\mu \rightarrow e\alpha$ was added to the fitting function for the spin-held data.
- Was obtaind the 90% confidence limits

- $\mathbf{R_{\alpha} < 2.6\ 10^{-6}}$
- $\eta_{\mu\mathbf{e}}$ $\mathbf{> 9.9\ 10^{9}}$ GeV

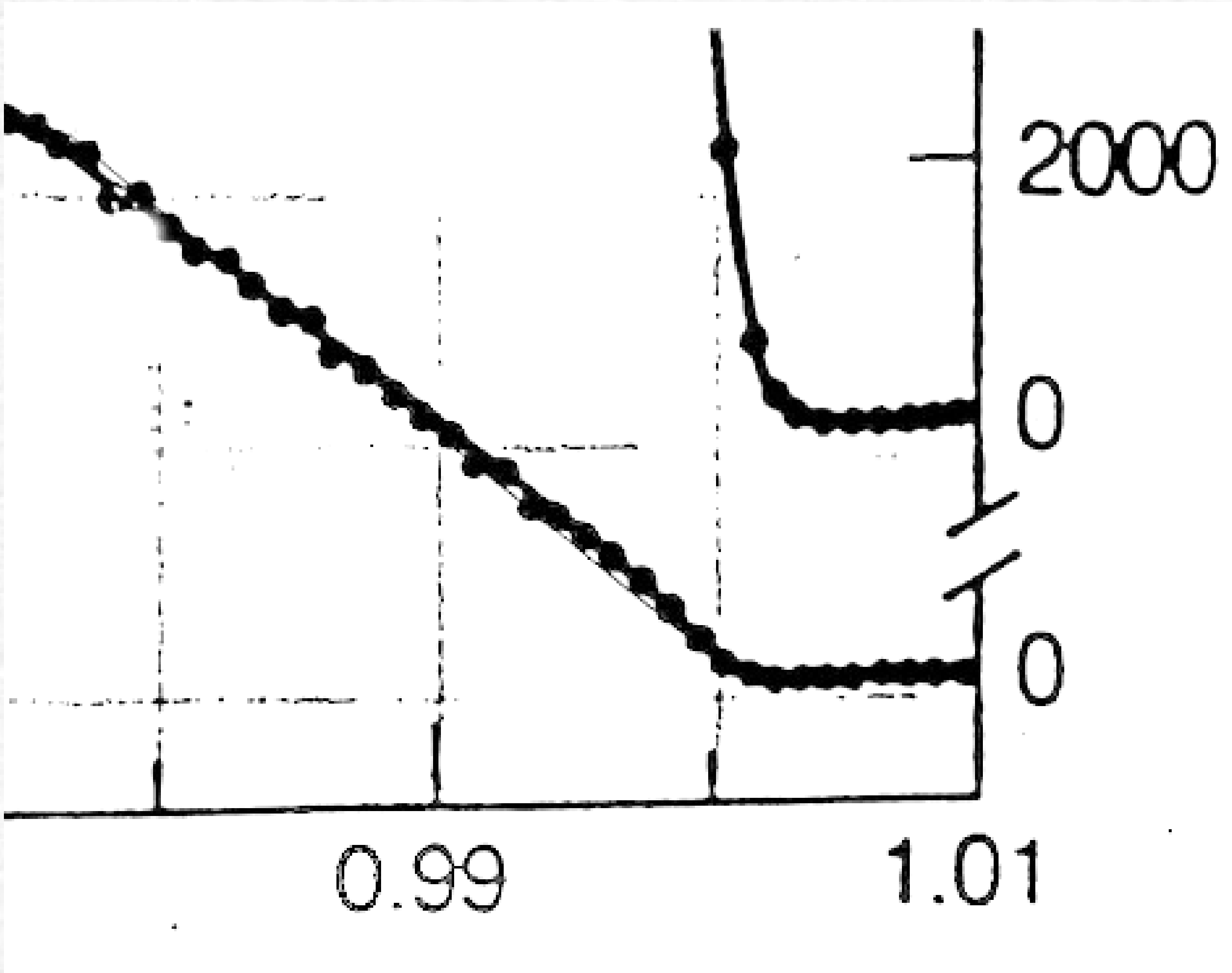
2000
0
0
0.99
1.01

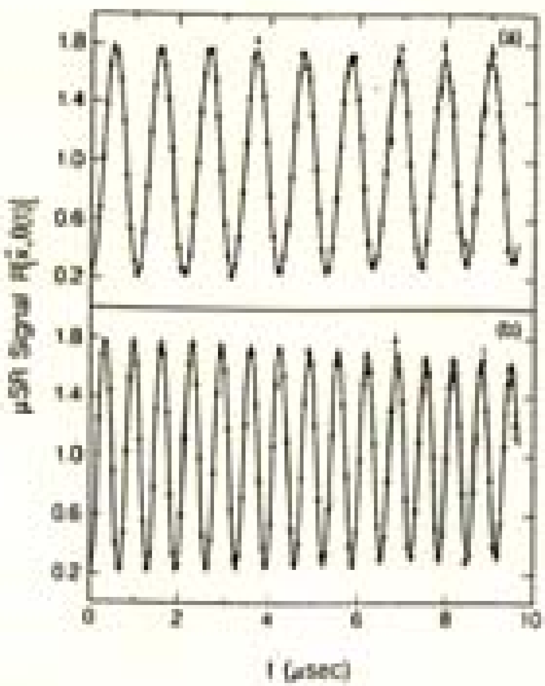

FIG. 1. Data from the second of three running periods, constituting 73% of the total μSR data, with (a) 70-G and (b) 110-G transverse fields. The exponential decay with μ^+ lifetime has been factored out.

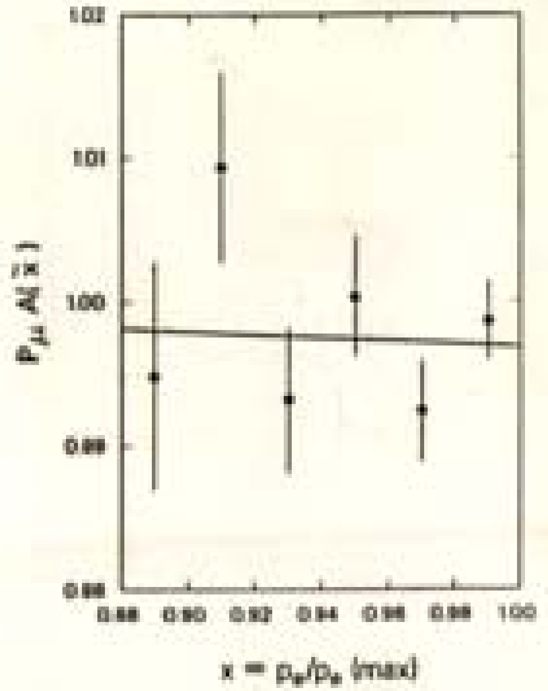

FIG. 4. Values of $P_\mu A(\bar{x})$ in each x bin for metal targets, excluding run-2 Cu. Error bars are statistical errors added in quadrature to the possible systematic error from the spectrometer momentum calibration. The line is a fit by Eq. (2) using world-average values of δ and ρ.

Crystal Box

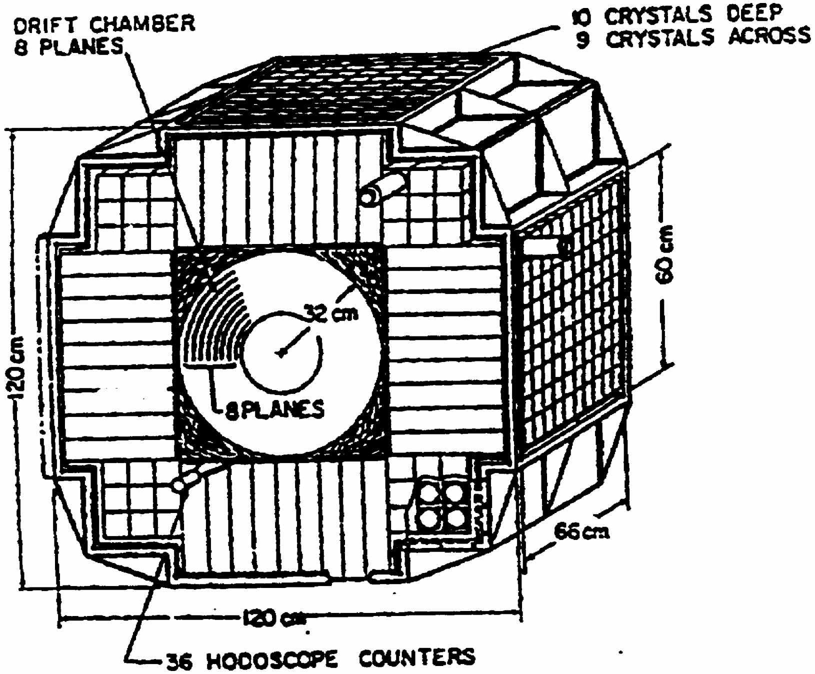

Рис. 5: Схема детектора Crystal Box[15].

для событий $\mu \to e\alpha\gamma$, $\mu \to e\bar{\nu}\nu\gamma$ и случайных совпадений, соответственно; x_i — вектор, компоненты которого равны M^2_{eff} и $\Delta t_{e\gamma}$.

Пик функции $L(n_{e\alpha\gamma}, n_{IB})$ расположен при значениях $n_{IB} = 7525 \pm 120$ и $n_{e\alpha\gamma} = 0$, что находится в хорошем согласии с ожидаемым значением числа $\mu \to e\bar{\nu}\nu\gamma$ – распадов в исследуемой мишени: $(n_{IB})_{\text{ожид}} = 7460 \pm 118(stat) \pm 800(syst)$.

Приведенные результаты для величины $R_{\alpha\gamma} = \Gamma(\mu^+ \to e^+\alpha\gamma)/\Gamma(\mu^+ \to e\bar{\nu}\nu)$ дают значение:

$$R_{\alpha\gamma} \leq 1{,}3 \cdot 10^{-9} \quad (90\% \text{ уровень достоверности}). \tag{3.12}$$

4 Анализ высокоэнергичной части спектра позитронов $\mu \to e$ – распада.

Прямое наблюдение пика от распада $\mu \to e^+\alpha$ на фоне распада $\mu \to e\bar{\nu}\nu$ помимо того, что требует магнитного спектрометра с высоким разрешением по энергии, связано и с многими трудностями абсолютных измерений — фоновые события, рассеяние и др.Однако, как показано в работах[17, 18], возможна такая постановка опыта по поиску распада $\mu^+ \to e^+\alpha$, где абсолютные измерения заменяются относительными.

Рассмотрим распады $\mu^+ \to e^+\alpha$ и $\mu^+ \to e^+\bar{\nu}\nu$ с точки зрения углового распределения позитронов относительно направления спина мюона. Из формул (3.5) и (2.6) видно, что если в первом случае имеет место изотропное распределение позитронов распада, то во втором — резко выраженная асимметрия вылета позитронов отно-

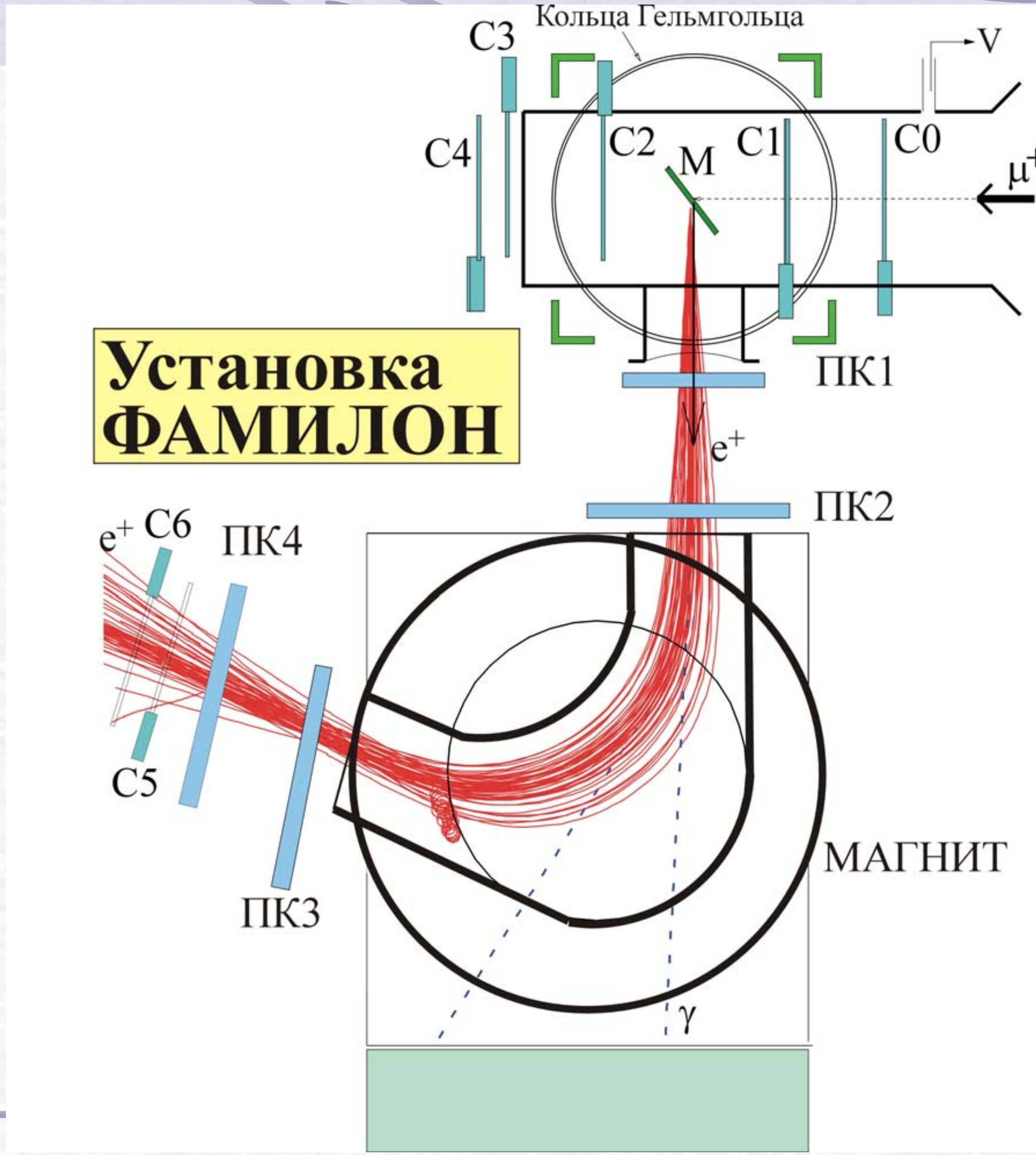
Кольца Гельмгольца
C3
V
C2
C1
C0
C4
M
μ^+
Установка ФАМИЛОН
ПК1
e^+
ПК2
e^+
C6
ПК4
C5
ПК3
МАГНИТ
γ


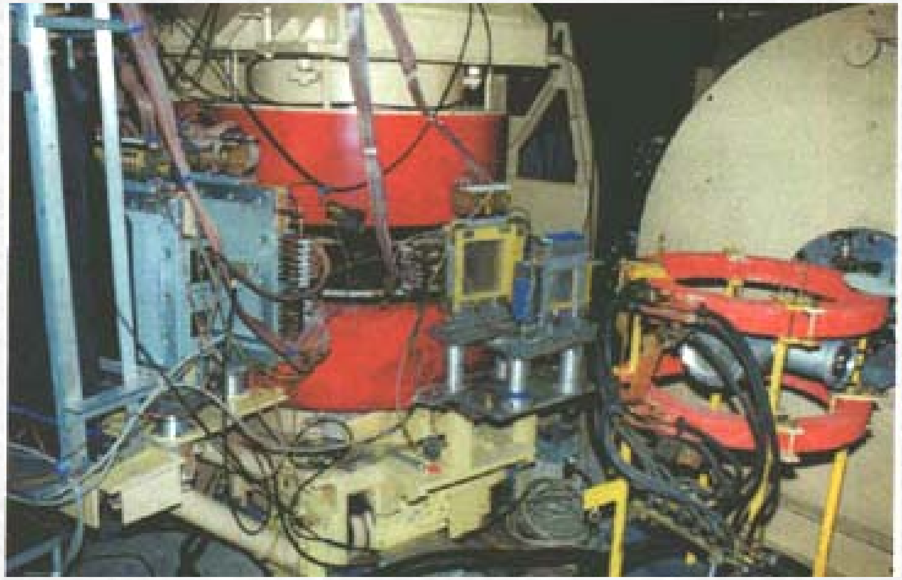
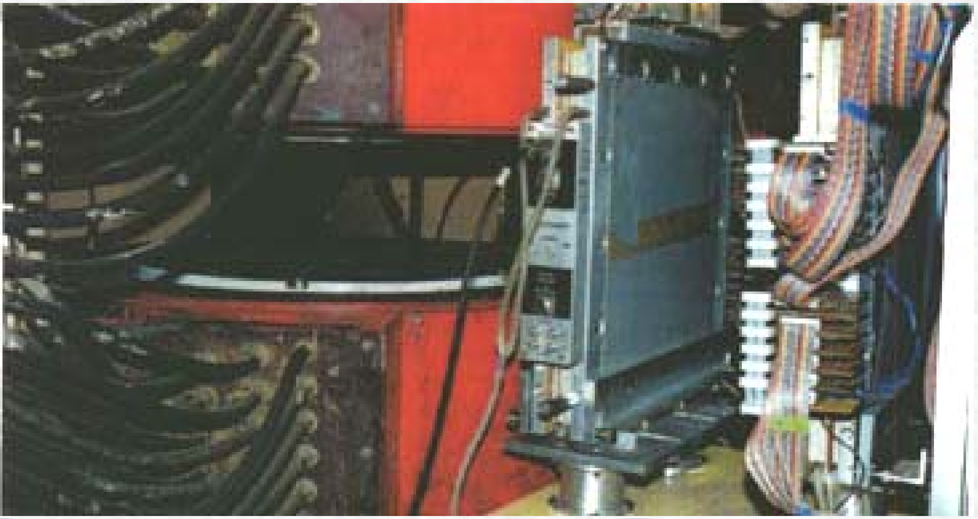
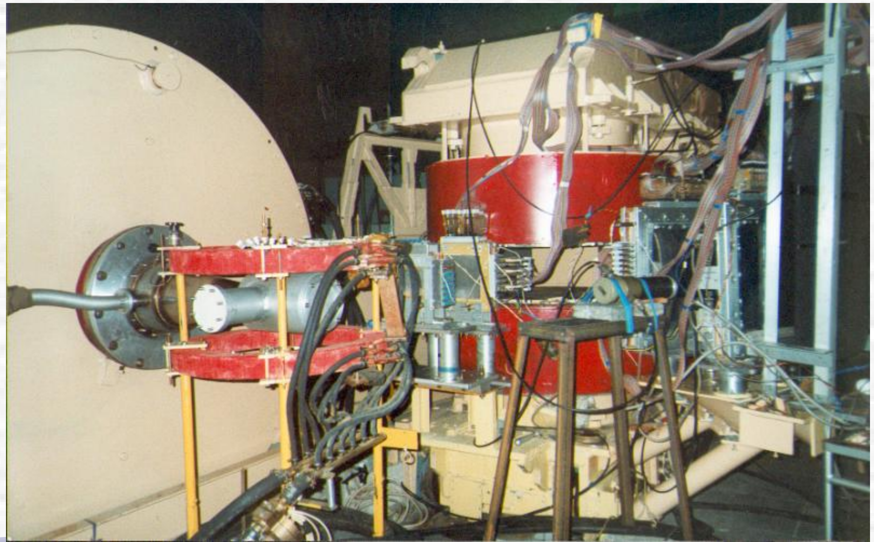

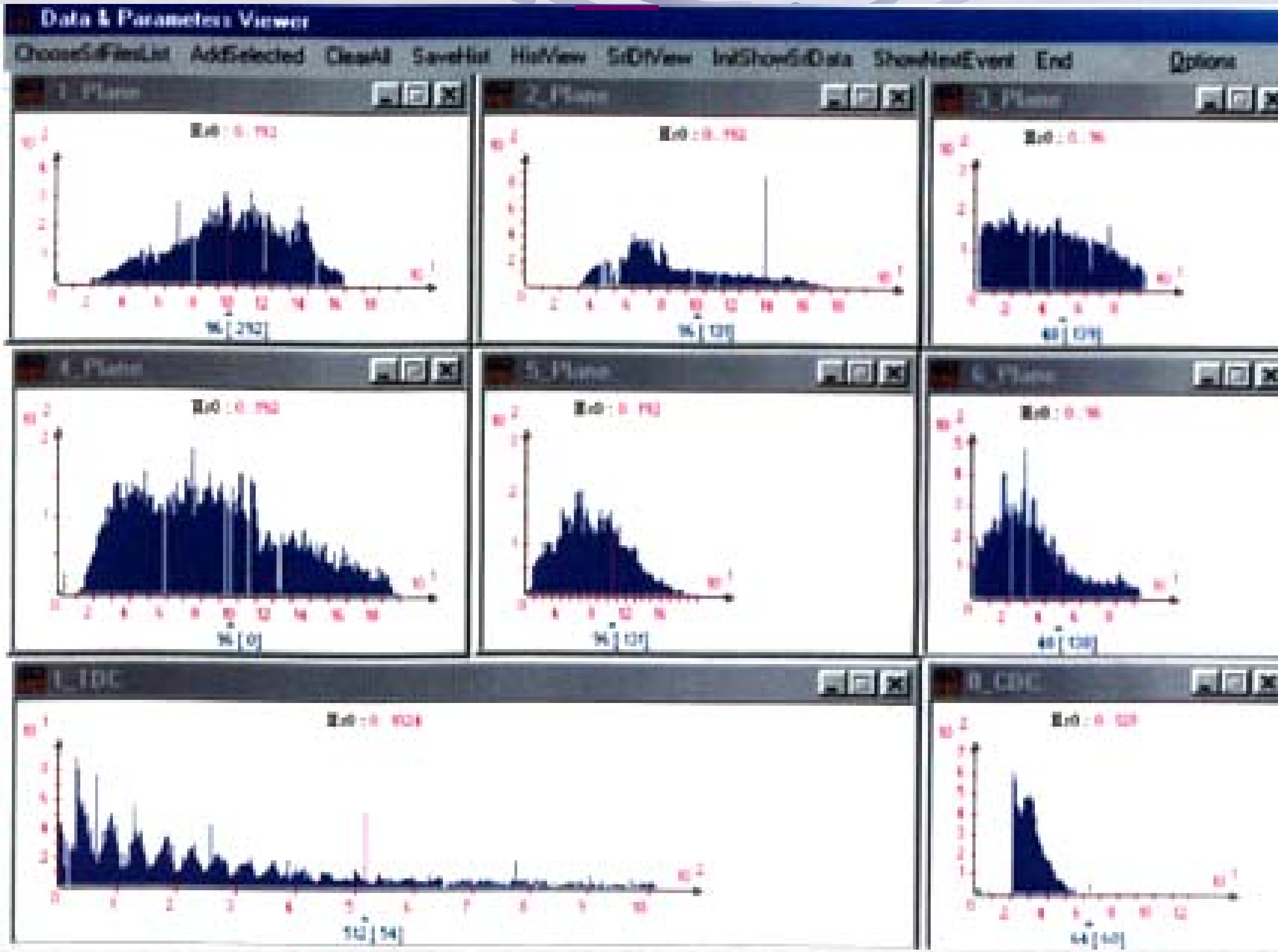

Data & Parameters Viewer
ChooseSdFilesList
AddSelected
ClearAll
SaveHist
HistView
SdDView
InitShowSdData
ShowNextEvent
End
Options

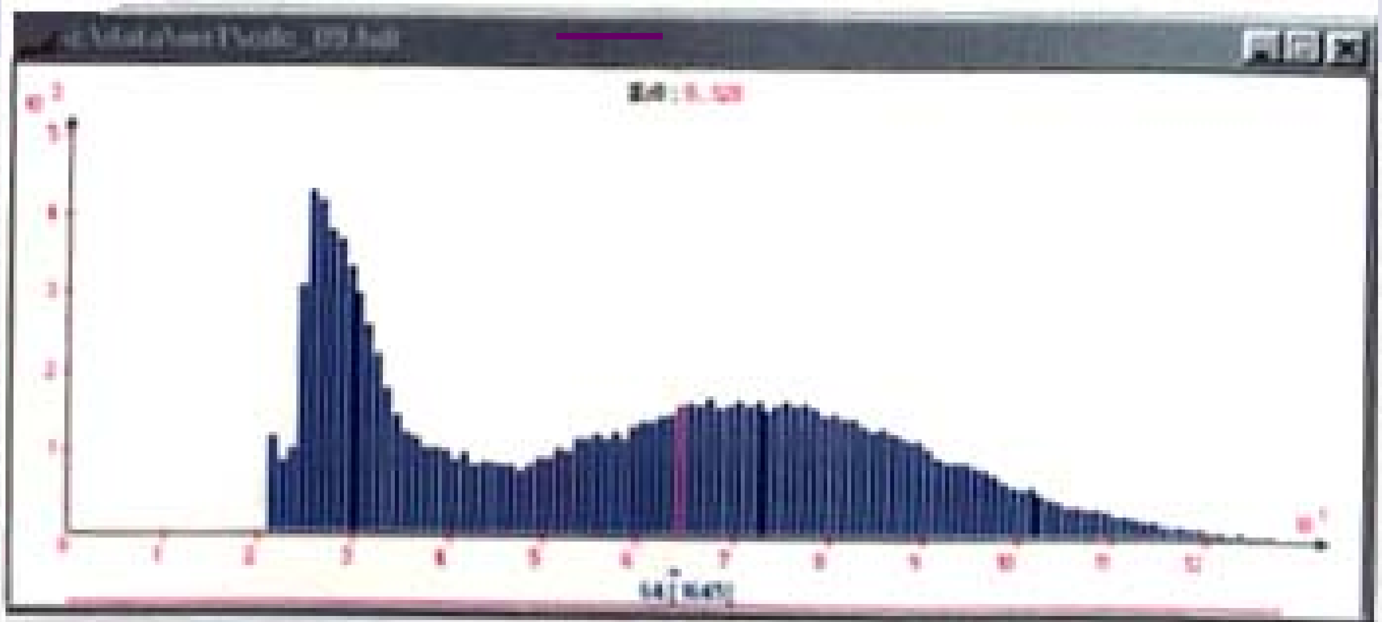

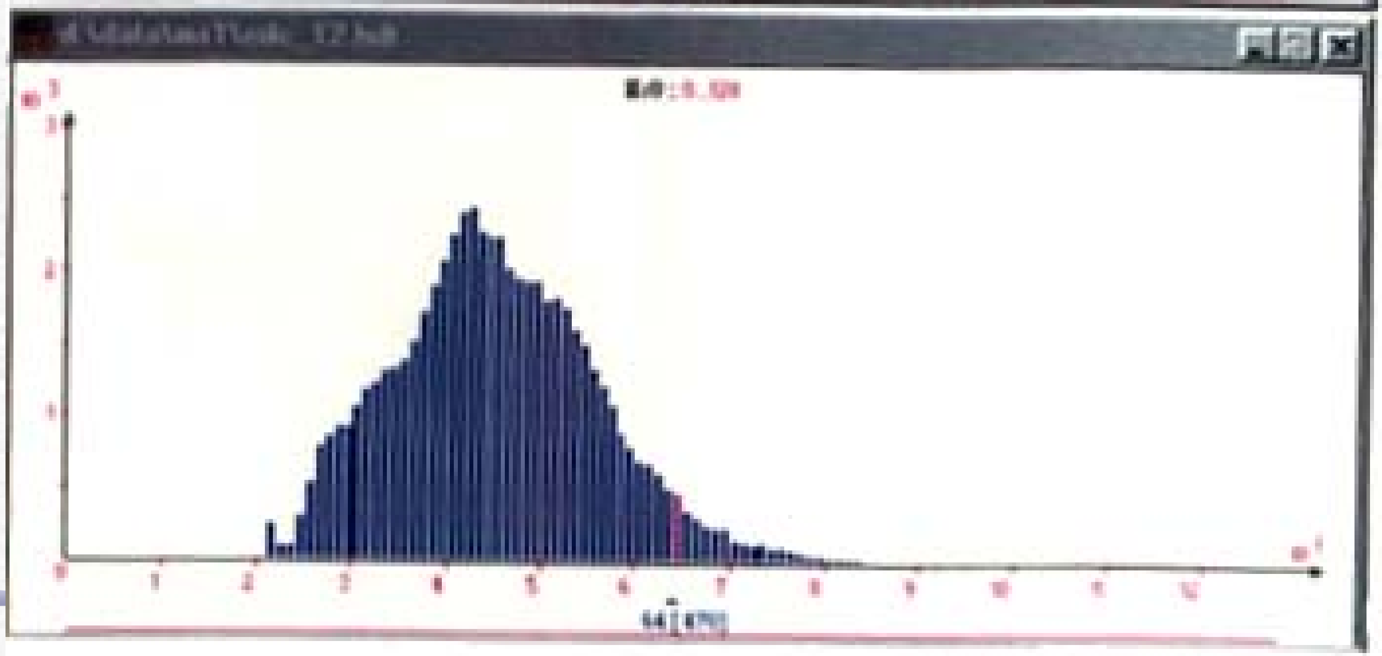

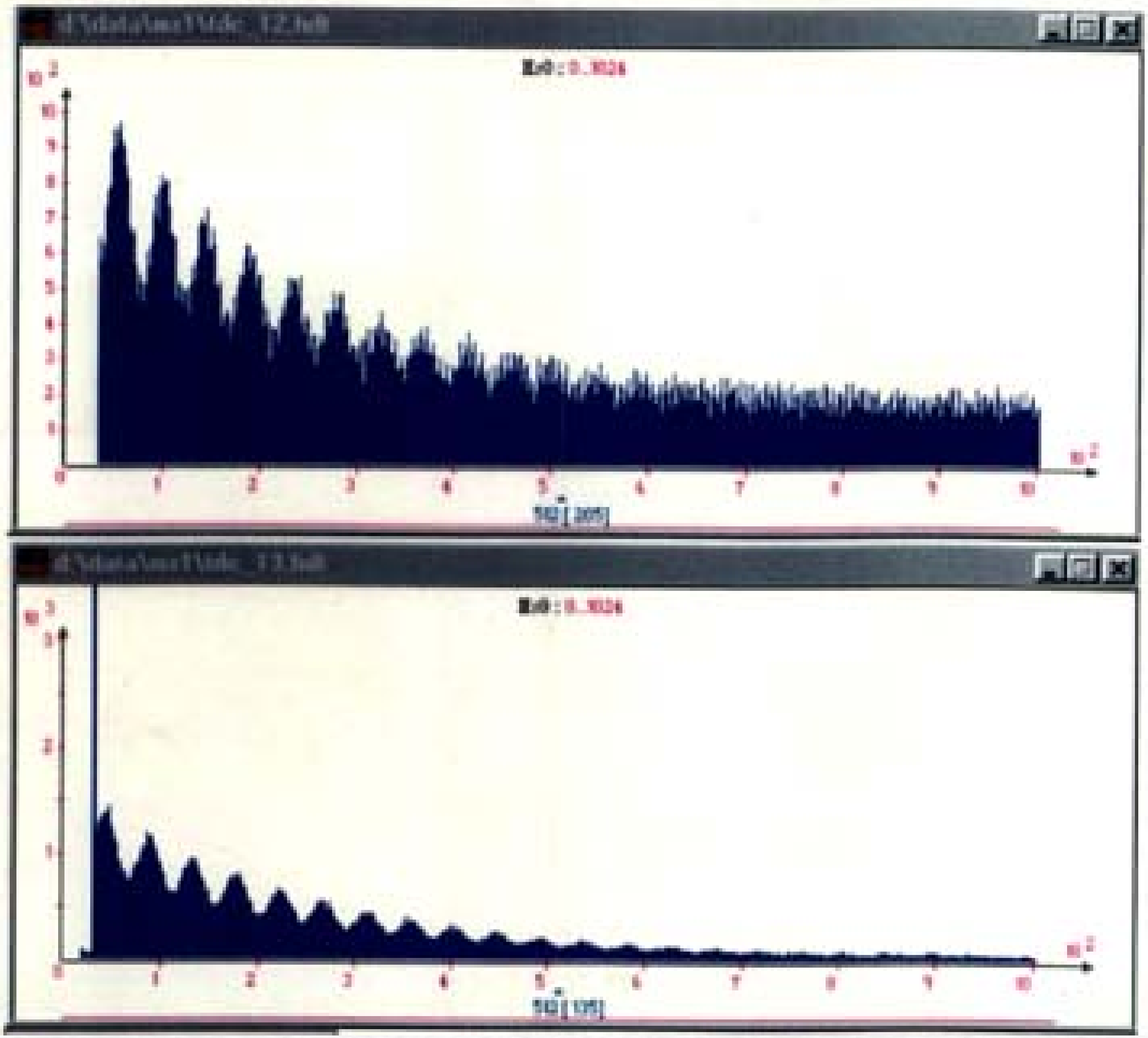

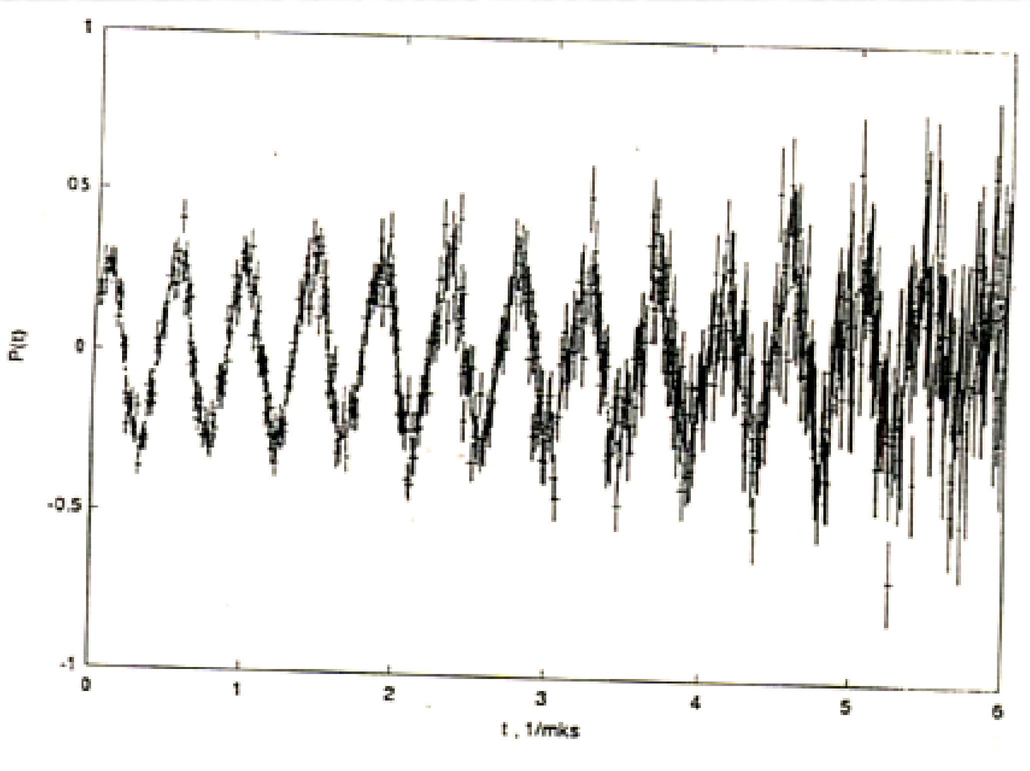

1
0.5
0
-0.5
-1
P(t)
0
1
2
3
4
5
6
t , 1/mks

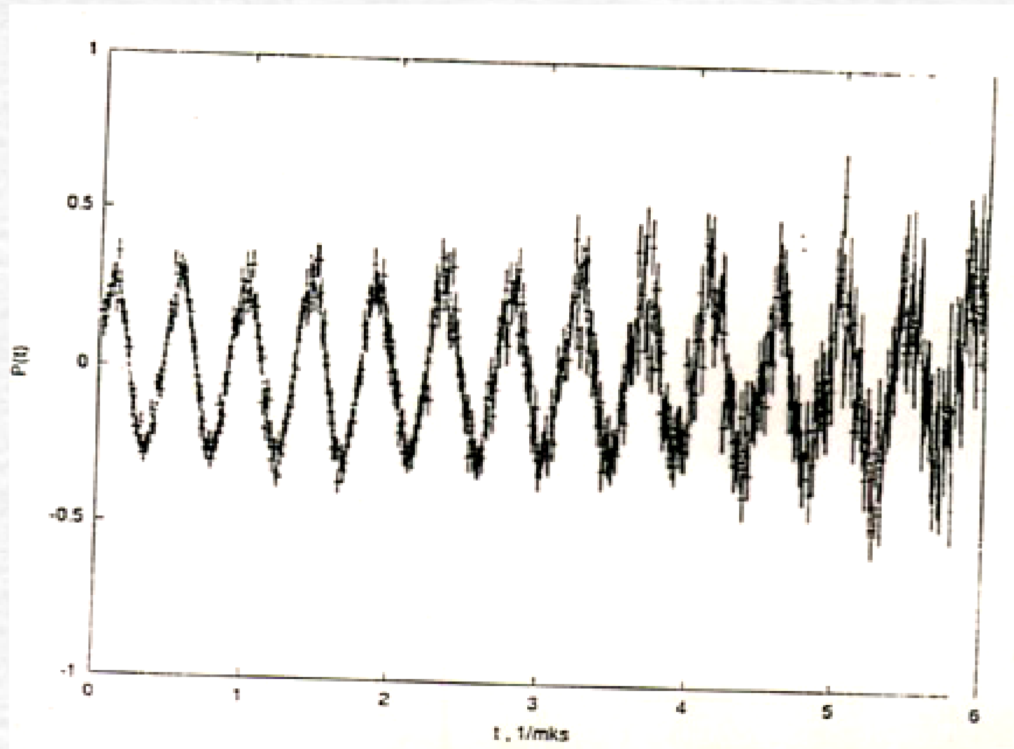

1
0.5
0
-0.5
-1
P(t)
0
1
2
3
4
5
6
t , 1/mks

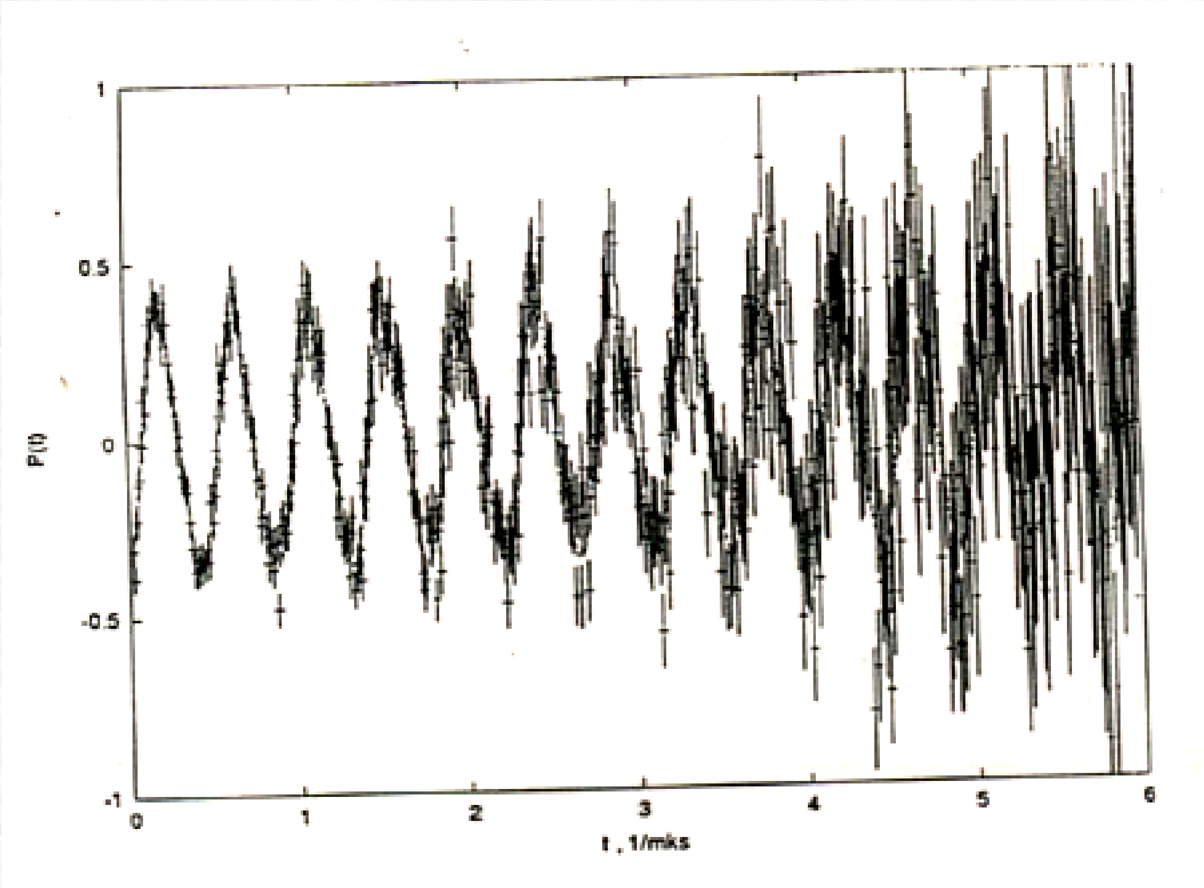

1
0.5
0
-0.5
-1
P(t)
0
1
2
3
4
5
6
t , 1/mks

----------------------------FAMILON------------------

--------------------- TEST RUN 30.05 - 2.06.201

	H Gauss	asymmetry		omega rad/mks		t0	f & L-ch		x^2	
1	164	.358	.005	14.047	.010	35.0	37	1000	975.1	tdc1_12.
2	164	.270	.003	14.007	.007	35.0	37	1000	1028.9	tdc1_13.
3	164	.276	.004	13.990	.009	35.0	37	1000	1037.4	tdc1_14.
4	164	.268	.004	14.021	.010	35.0	37	1000	1186.6	tdc1_15.
5	164	.510	.007	13.887	.009	35.0	55	1000	1196.7	summary_

State Scientific Center of Russian Federation

Institute for Theiretical and Experimental Physics

(ITEP)

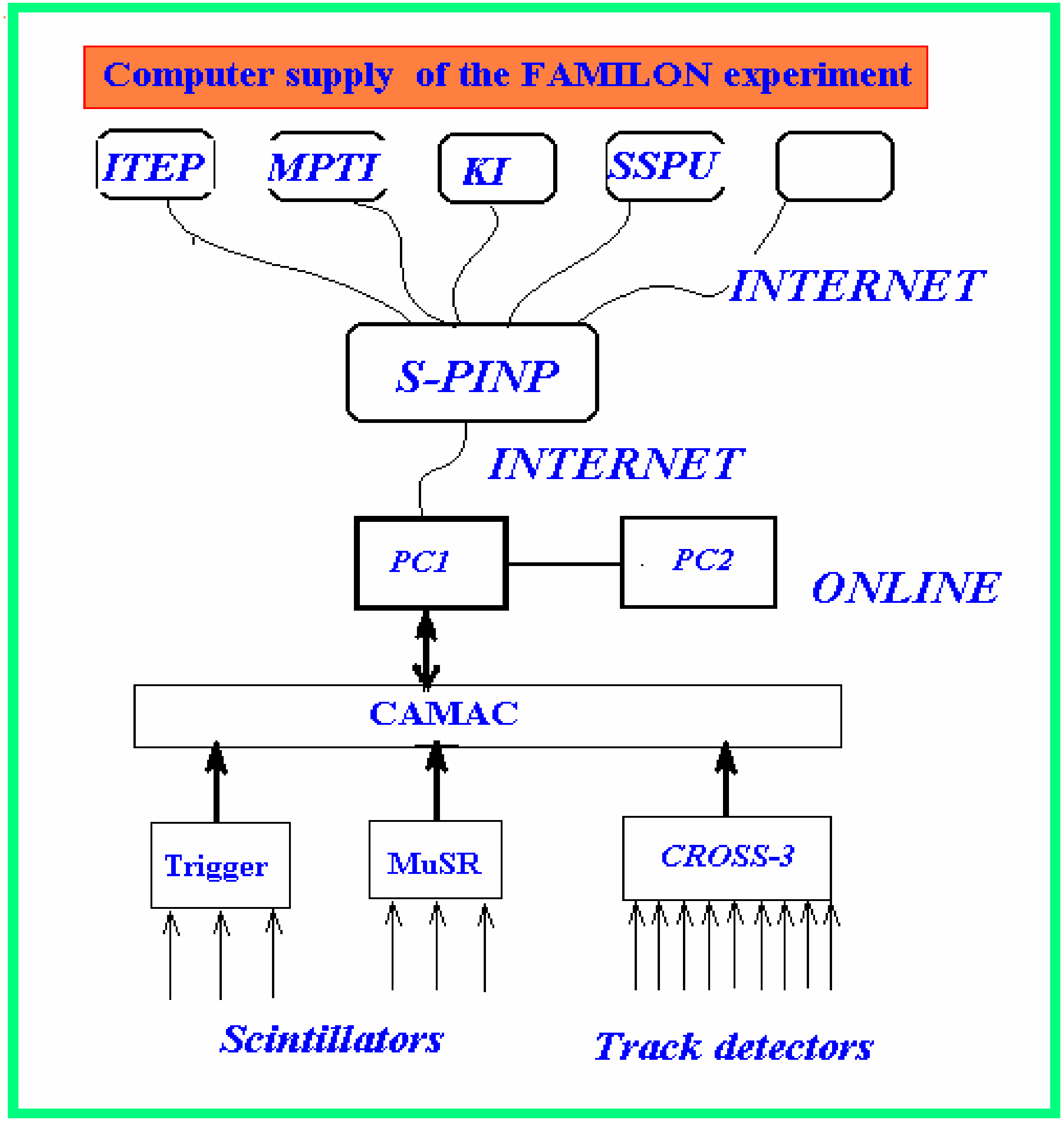
Computer supply of the FAMILON experiment
ITEP
MPTI
KI
SSPU
INTERNET
S-PINP
INTERNET
PC1
PC2
ONLINE
CAMAC
Trigger
MuSR
CROSS-3
Scintillators
Track detectors

The aims of simulation procedure were:

1. Optimization of the geometry arrangement of the set-up elements.

2. Analysis of the action of the density substances along the positron trace.

3. Evaluation of the positron momentum measurement precision.

4. Calculation of the positron detection efficiency.

FAMILON Full Scale Simulation

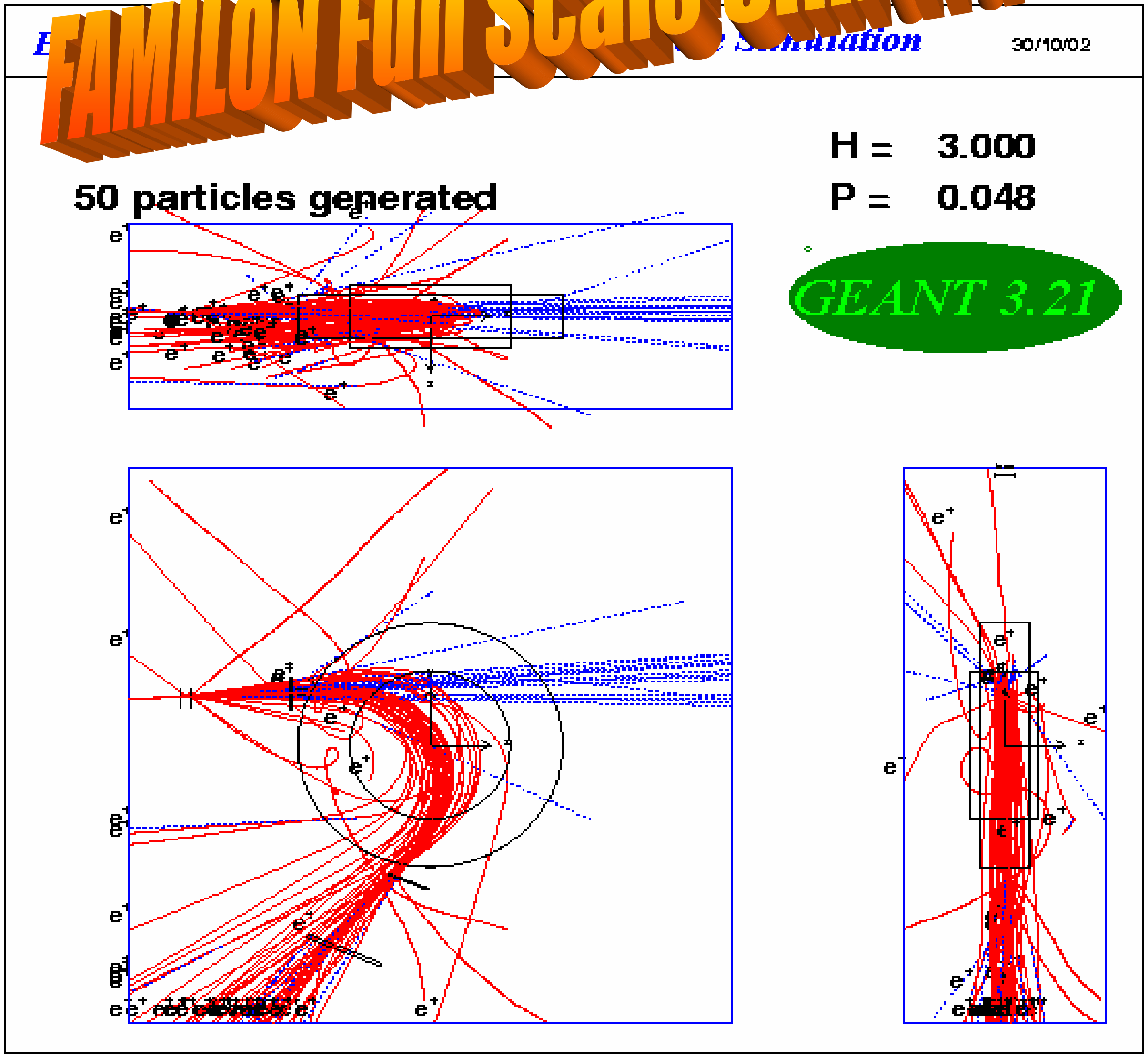

FAMILON: Angle measurement precision

defines the distance between blocks of prop. chambers bihind magnet.

Two factors must be taken into account:

1. Errors in measuring of coordinates due to discrete disposition of sensitive wires in proportional chambers.

2. Positron multiple scuttering in air between the chamber samples.

Both factors depends on distance between the samples.

Optimal distance is determined by the minimum of the total presicion.

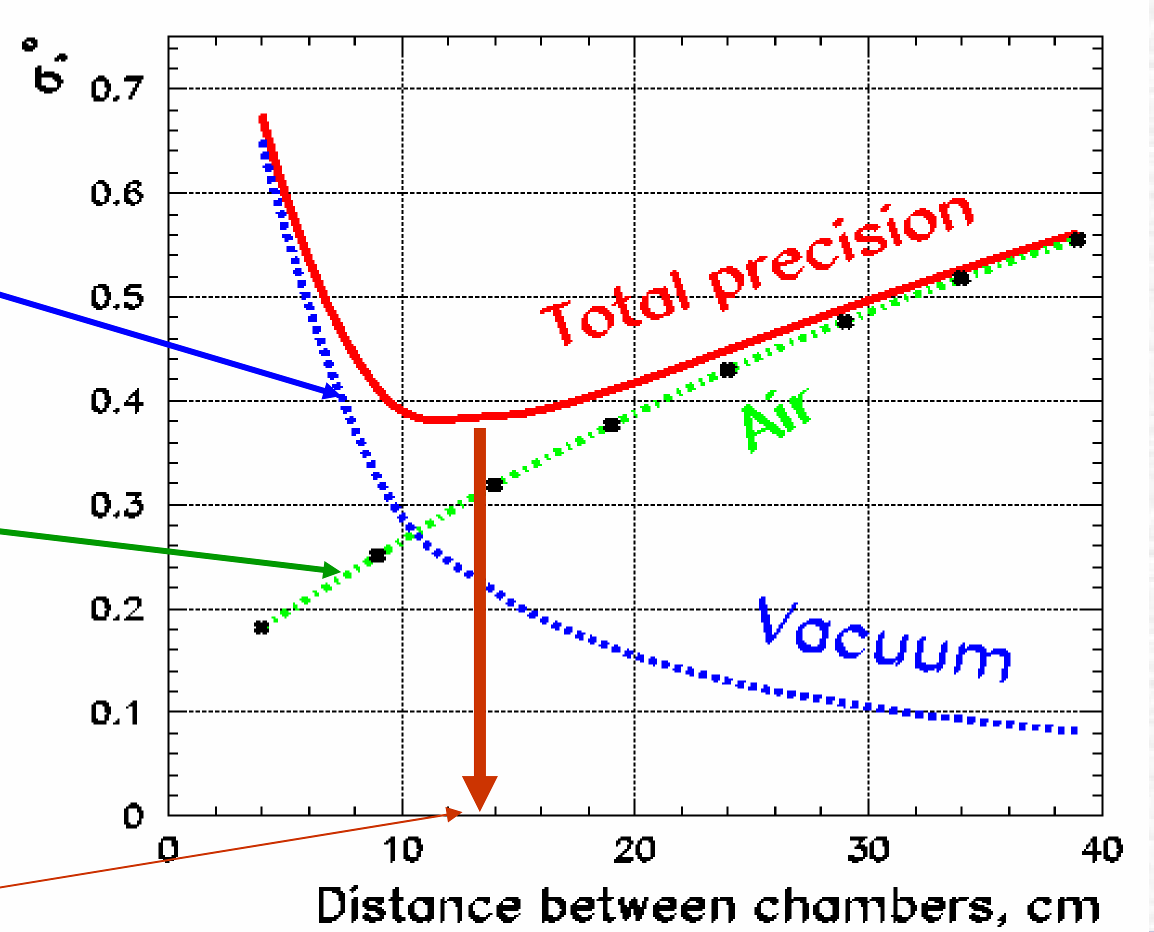

Coordinates measurement precision

Momentum measurement precision is determined by coordinate precision

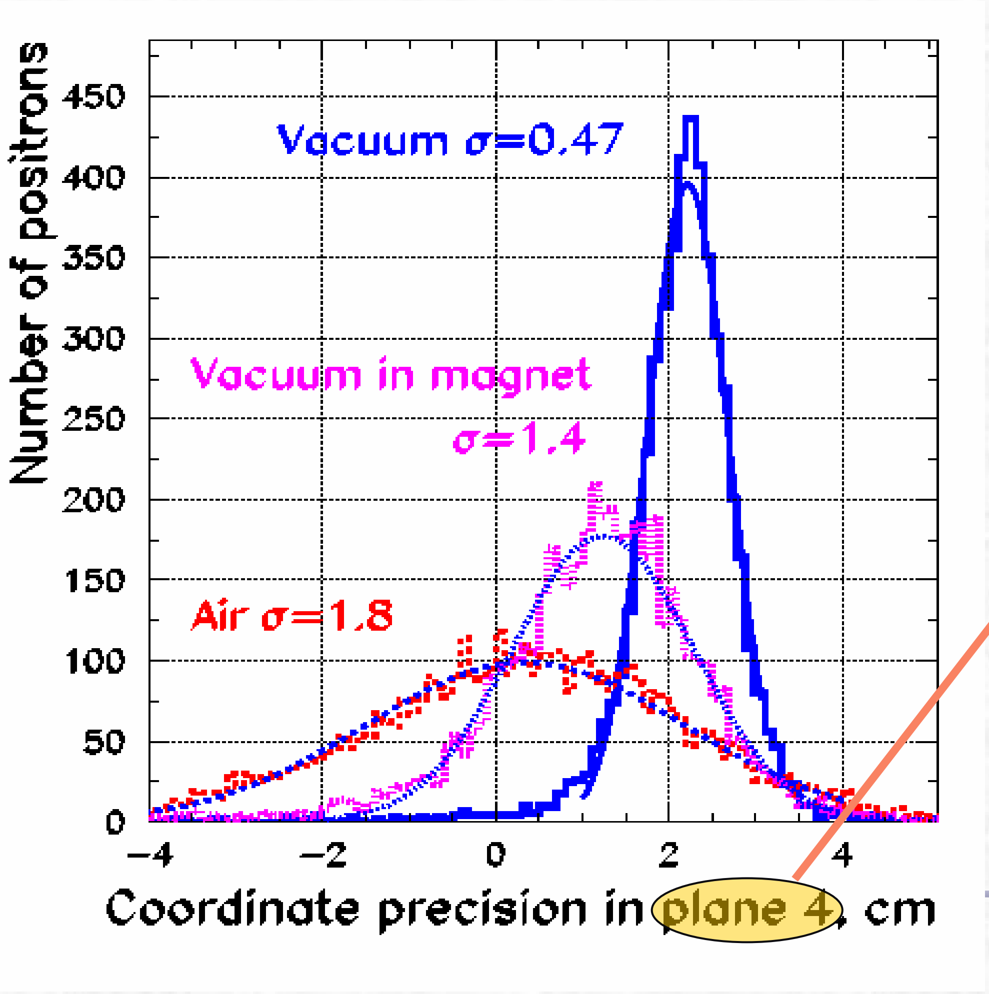

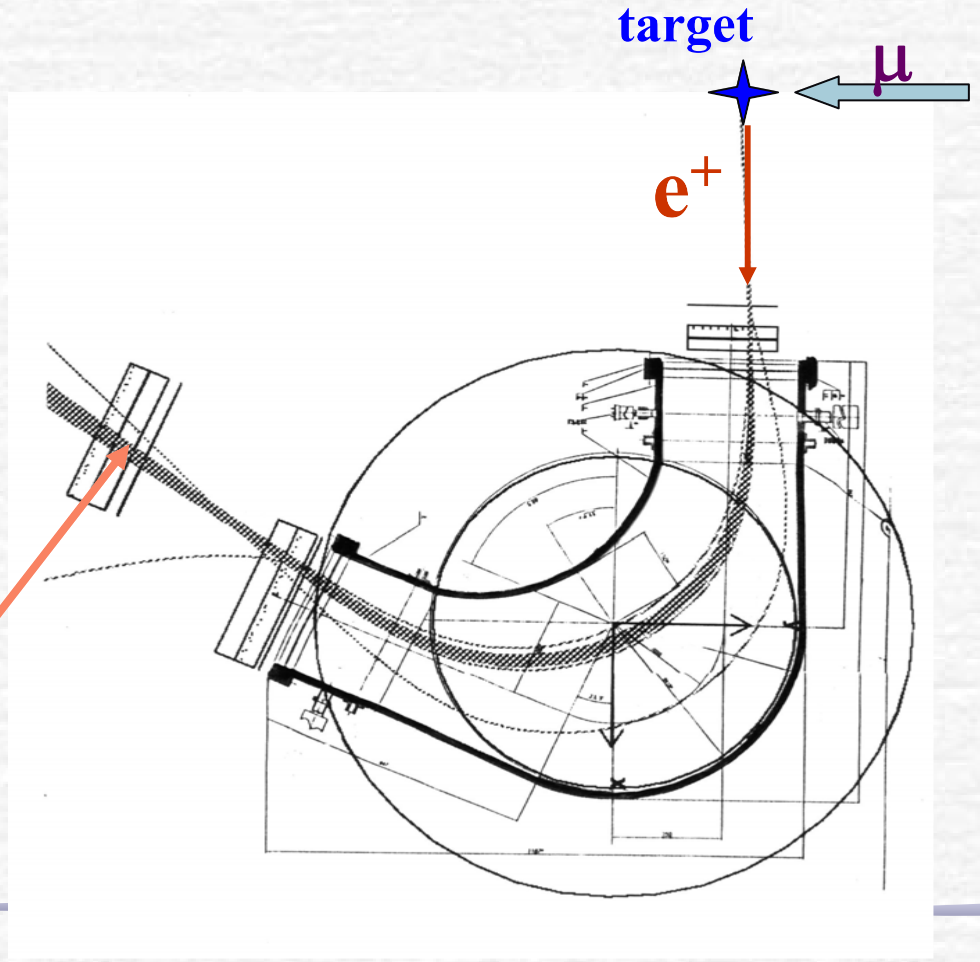

Motne Karlo efficiency evaluation

Efficiency of positron registration ε depends on energy E and angle θ of positron $\varepsilon = F(E, \theta)$.

ε is defined by geometrical disposition of the magnetic spectrometer elements: size of the magnetic field region, scale and location of the proportional chambers and distance between the target and spectrometer.

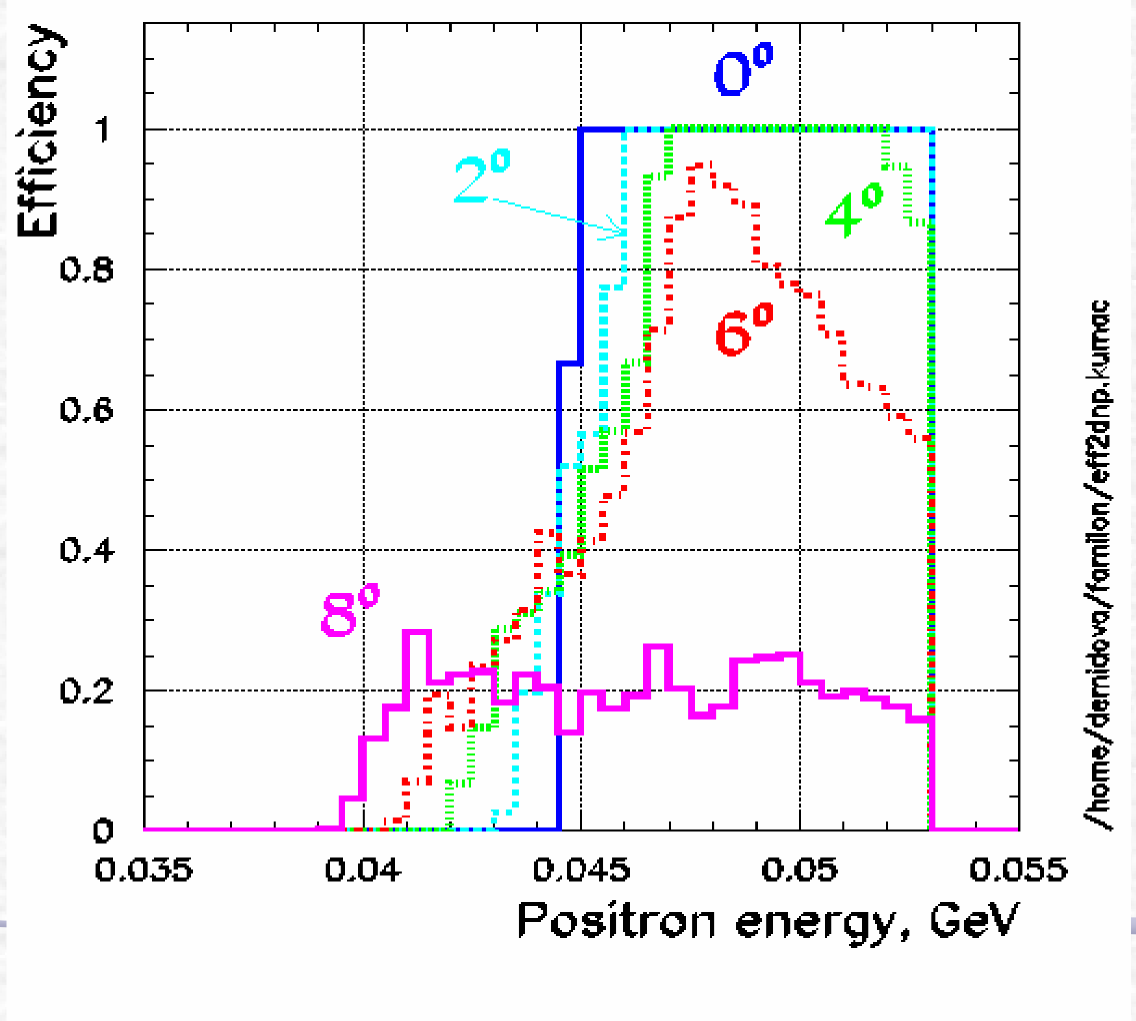

The results of the methodical run are demonstrated the conformity of the realized *simulation*

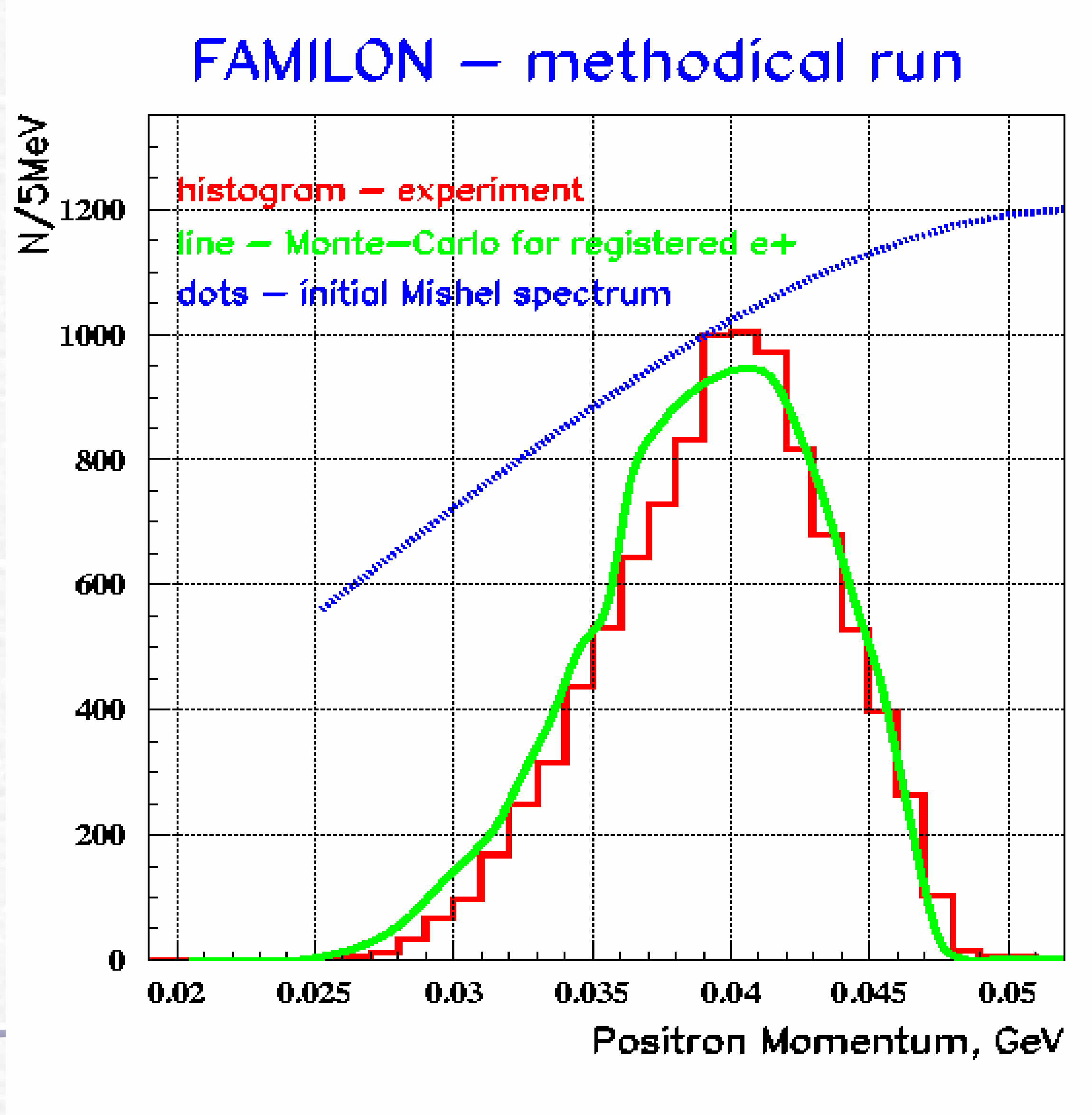

Predicted relative precision σ_P/P of the positron momentum measurement for different Sut-up modification.

1. Extreme precision (vacuum elswhere) -	$5\ 10^{-4}$
2. Maximal precision for the avaliable design of proportional chambers (vacuum + 3 plane of the) -	$2.5\ 10^{-3}$
3. Vacuum only in inside of the magnet -	$5\ 10^{-3}$
4. Helium elswhere -	$3\ 10^{-3}$
5. Air elswhere -	$9\ 10^{-3}$
6. Vacuum inside of the magnet, helium in the residual volume -	***$2.6\ 10^{-3}$***

LHC

CMS

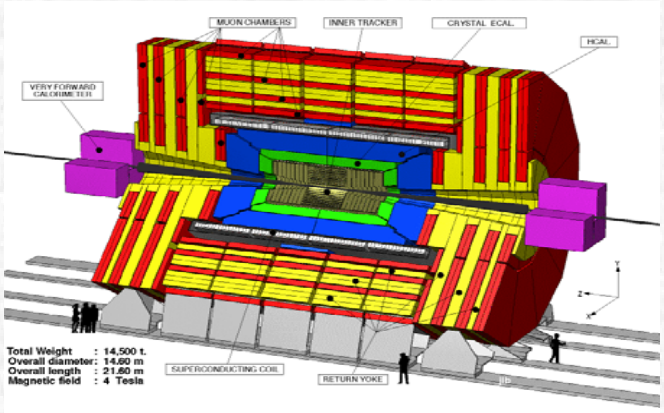

ATLAS

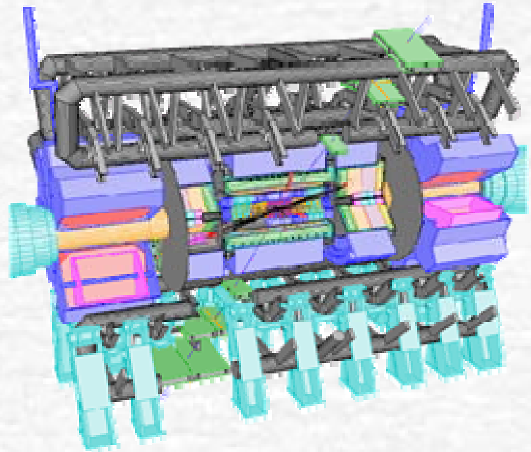

LHCb

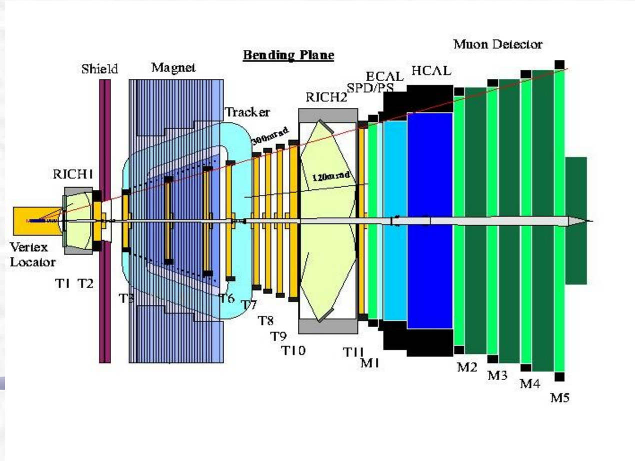

ALICE

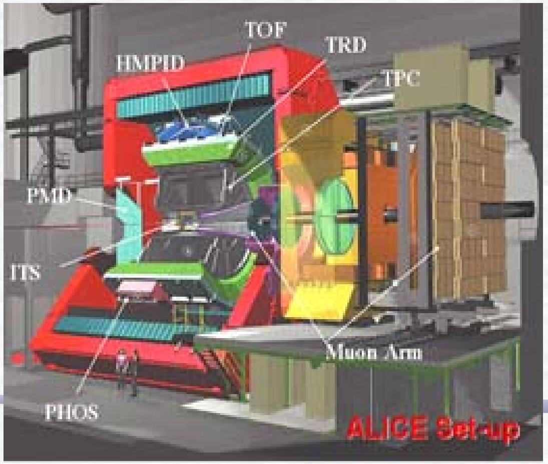

CMS

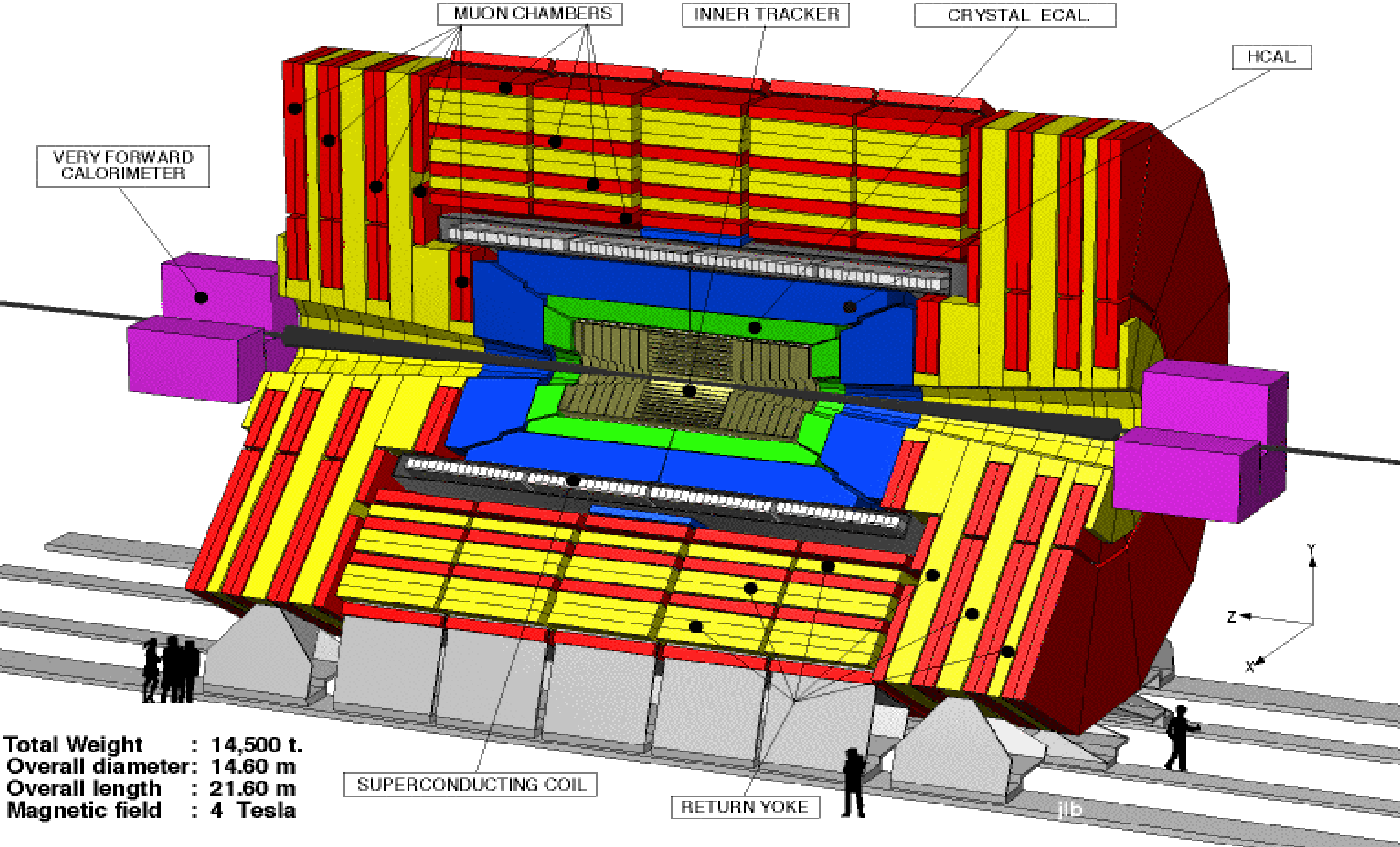

Total Weight : 14,500 t.
Overall diameter: 14.60 m
Overall length : 21.60 m
Magnetic field : 4 Tesla

Пияф должен был изготовить 120 6-слойных камер

500 000 анодных нитей

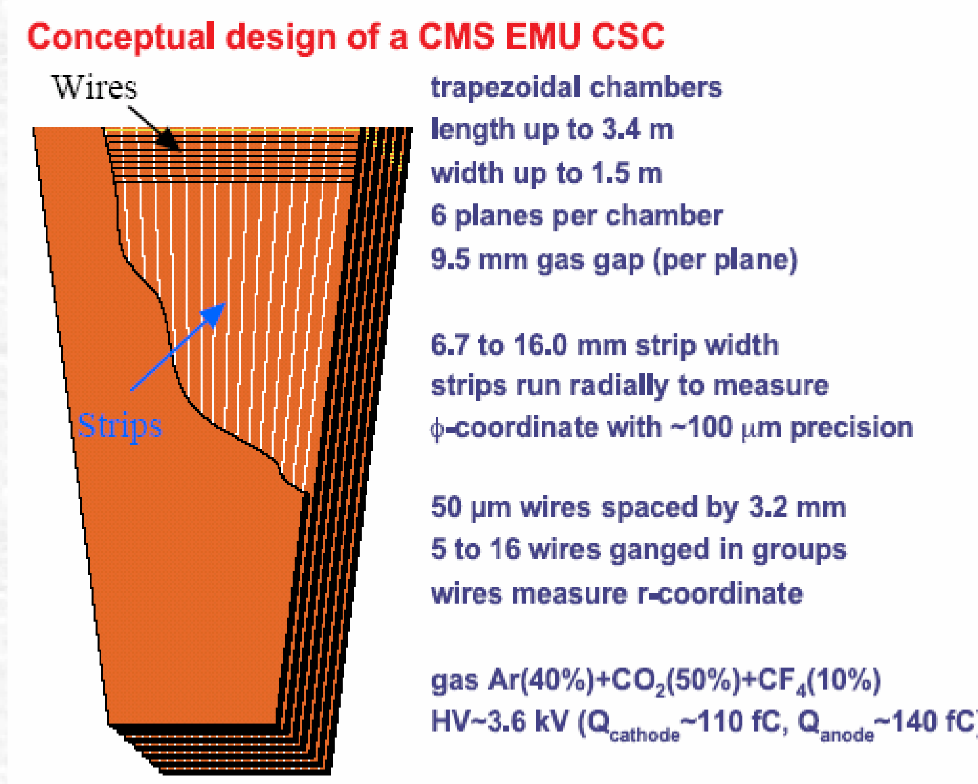

CSC Production at PNPI

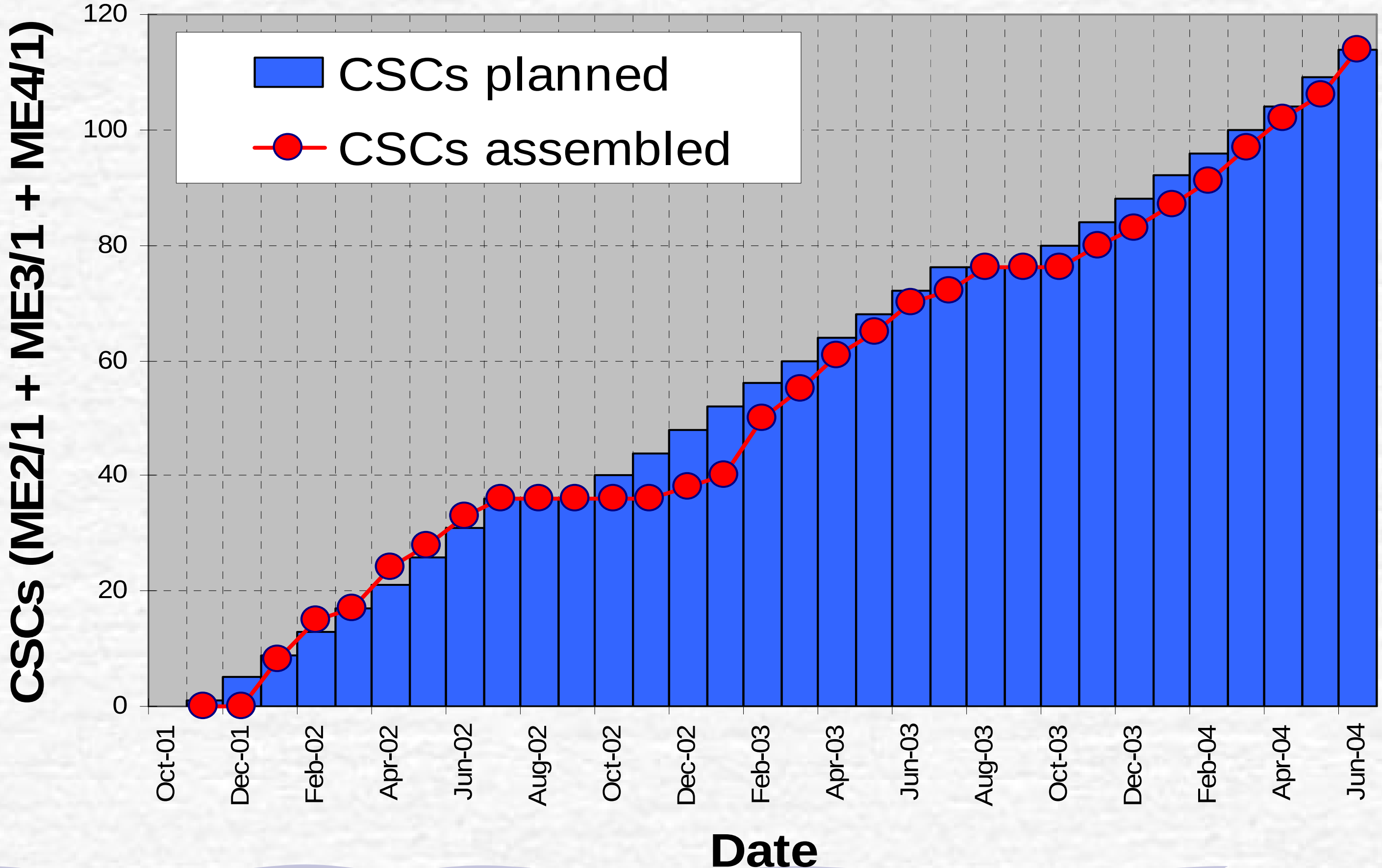

PNPI CSC Factory






Assembling with electronics

PNPI Fast Site

Transportation to CERN

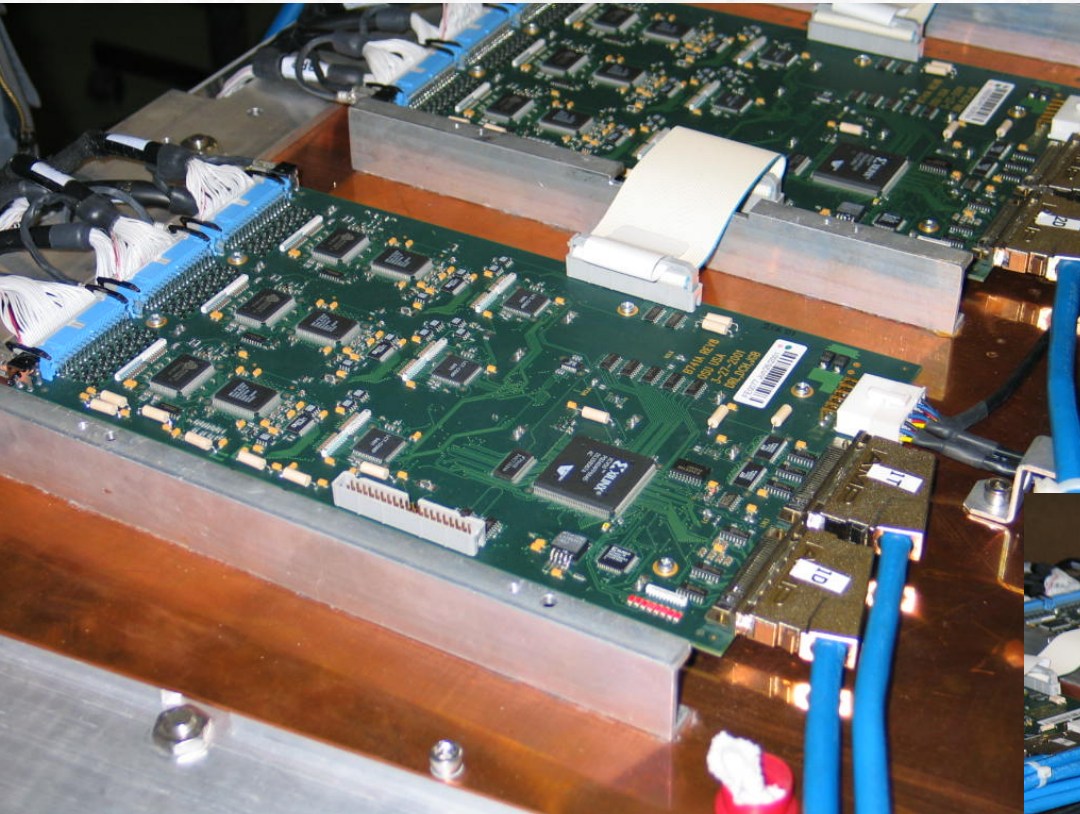

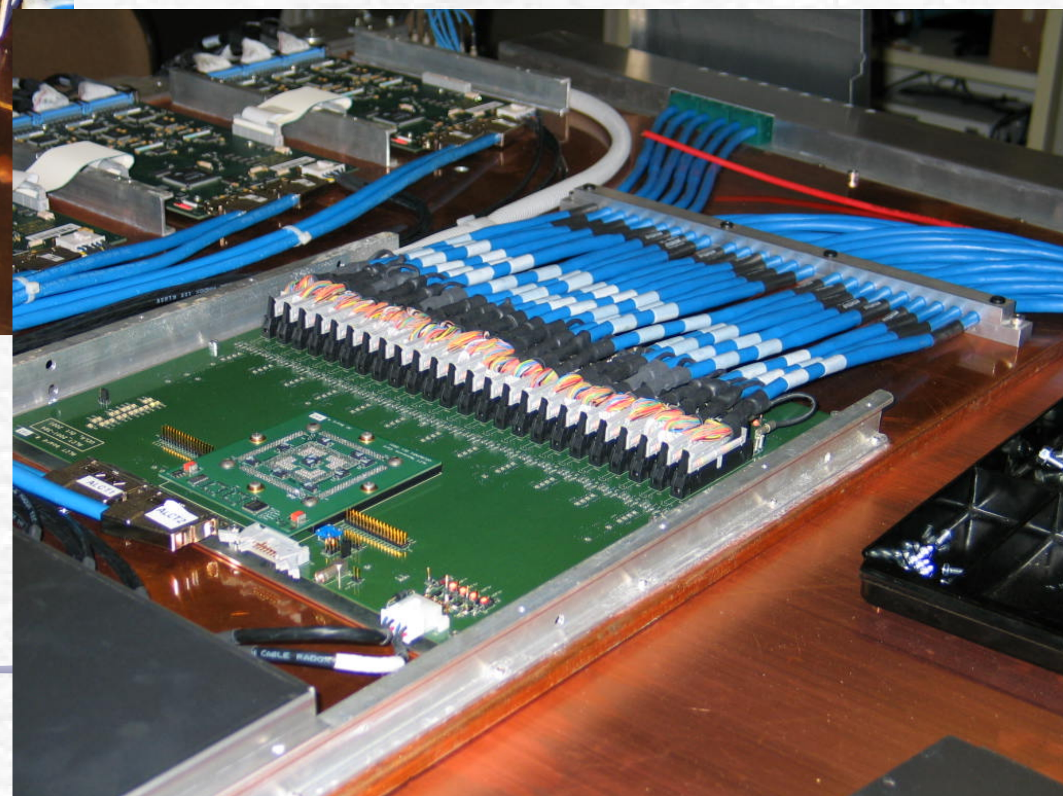

CROS3 Координатная Система С[illegible]ния

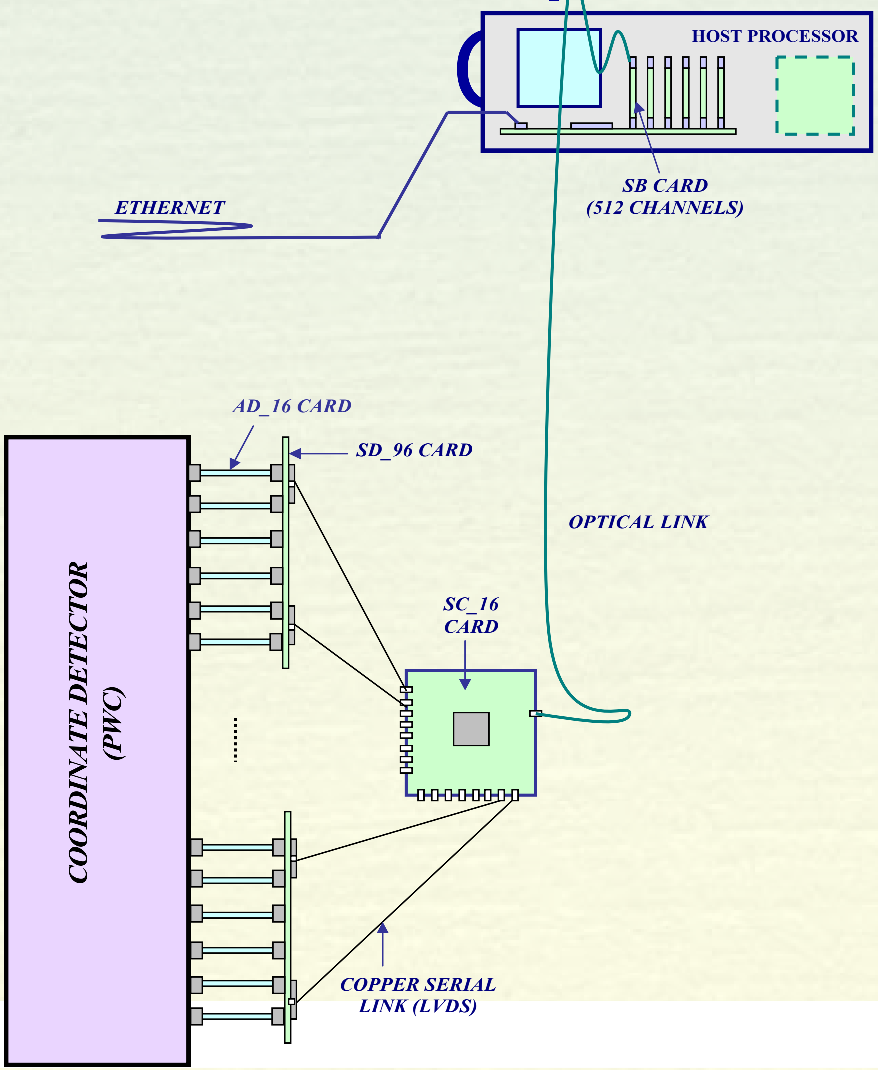

AD_16 – 16-канальный усилитель-дискриминатор

SD_96 – Системный модуль синхронизации, задержки и кодирования

SC_16 – Системный концентратор данных

SB- Системный буфер и интерфейс

CROS3 Координатная Система Считывания

CROS3 – прототип координатной системы считывания, разрабатываемый с 2003

Учитывает достоинства (и недостатки) предыдущих систем CROS, CROS2

Использует достижения современных технологий интегральных микросхем в том числе – ASIC CMP16_g и FPGA Xilinx Spartan II

Особенности системы:

**** Предусилитель, дискриминатор, задержка и считывание расположены непосредственно на детекторе***

**** Быстрое кодирование и считывание данных с частотой 40 MHz***

**** Возможность измерения временного распределения срабатывания каналов в интервале «ворот» схемы совпадений с дискретностью до 2.5 ns***

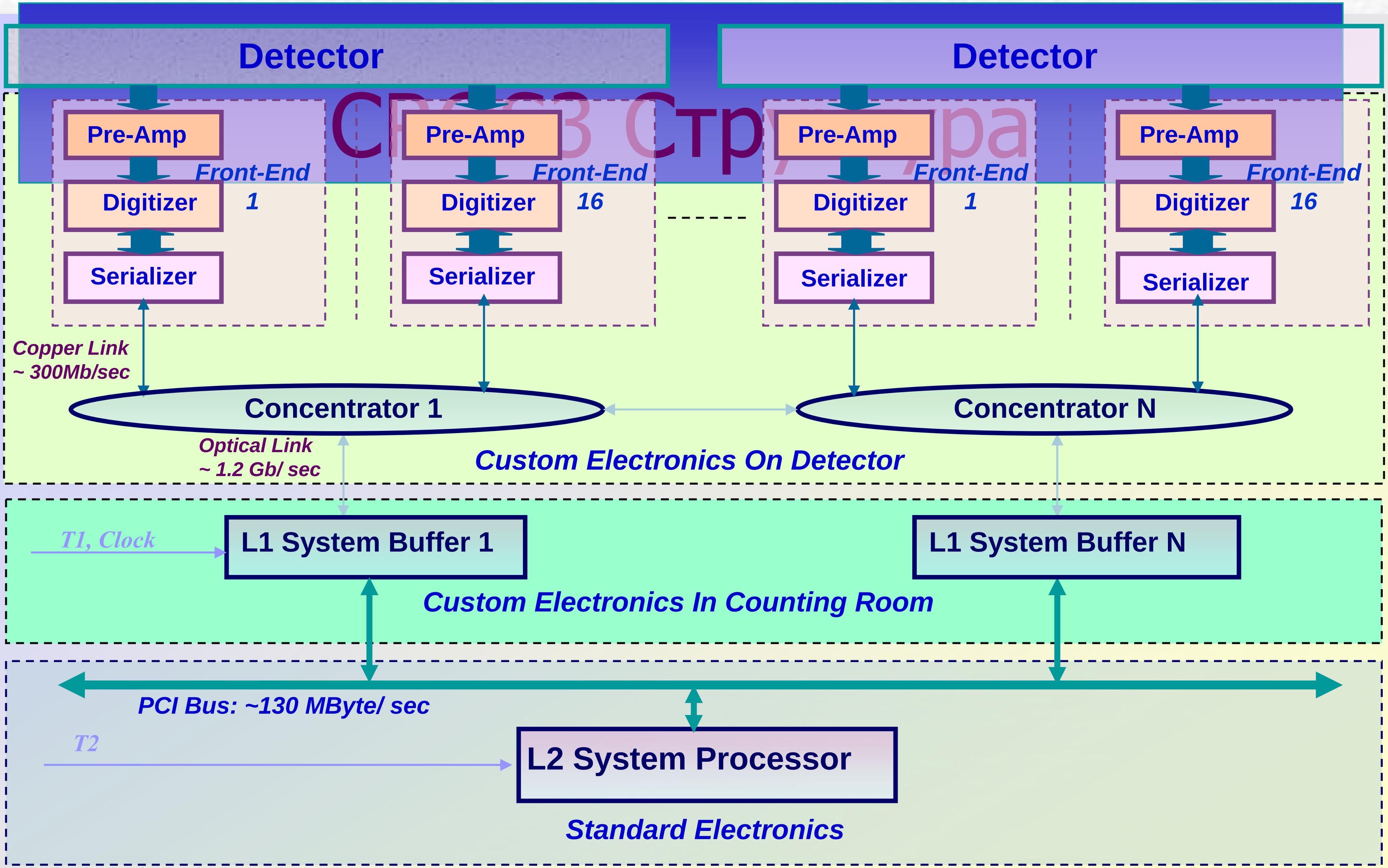
Detector
Detector
Pre-Amp
Pre-Amp
Pre-Amp
Pre-Amp
Front-End
Front-End
Front-End
Front-End
Digitizer
Digitizer
Digitizer
Digitizer
1
16
1
16
Serializer
Serializer
Serializer
Serializer
Copper Link
~ 300Mb/sec
Concentrator 1
Concentrator N
Optical Link
~ 1.2 Gb/ sec
Custom Electronics On Detector
T1, Clock
L1 System Buffer 1
L1 System Buffer N
Custom Electronics In Counting Room
PCI Bus: ~130 MByte/ sec
T2
L2 System Processor
Standard Electronics

CROS3_PWC Архитектура

1000 Channel in 2005
Parameters:
Delay 10 – 1280 ns Gate 10 – 640 ns Trigger Rate ~100KHz

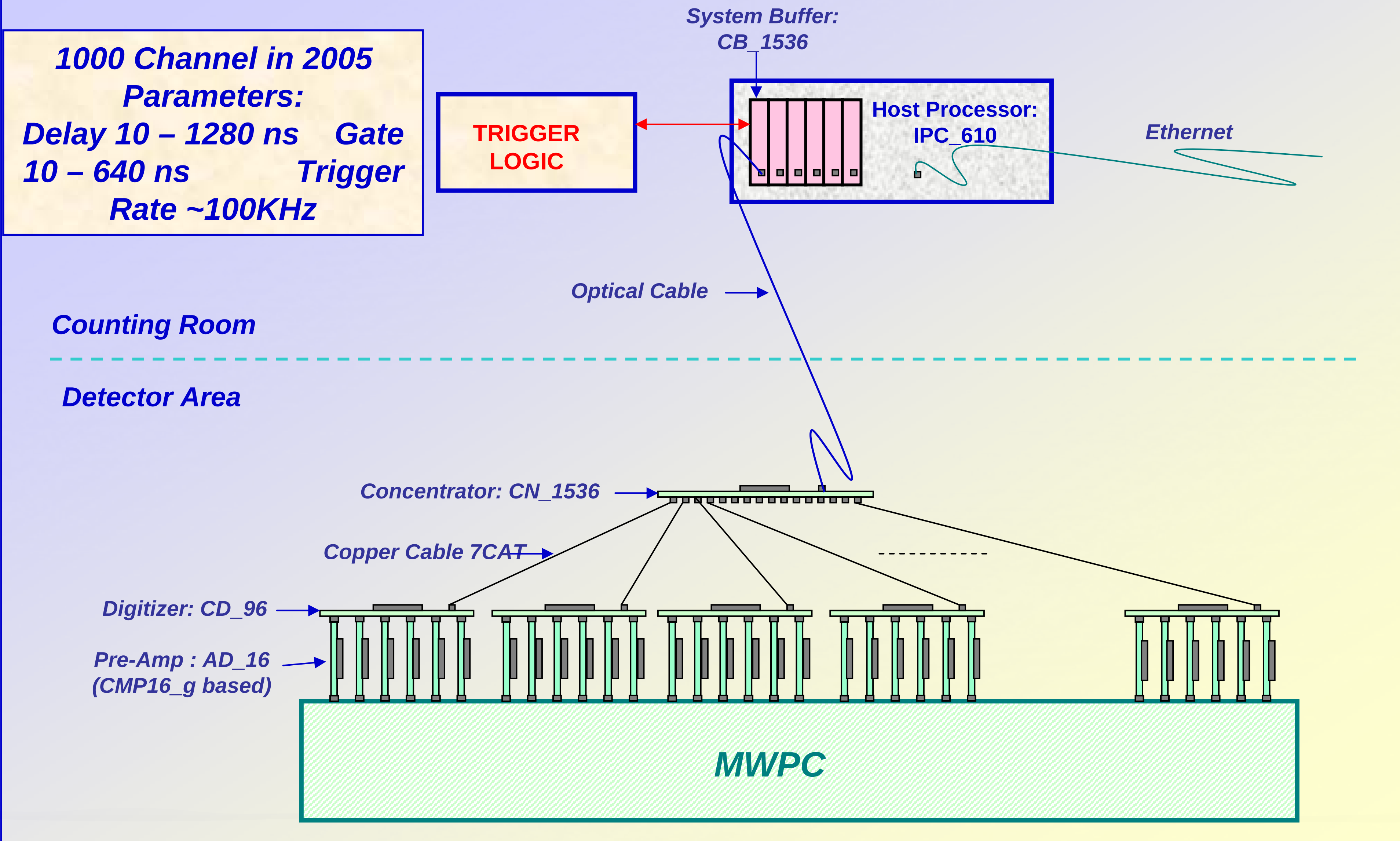

Энергетический разброс пучка после мишени

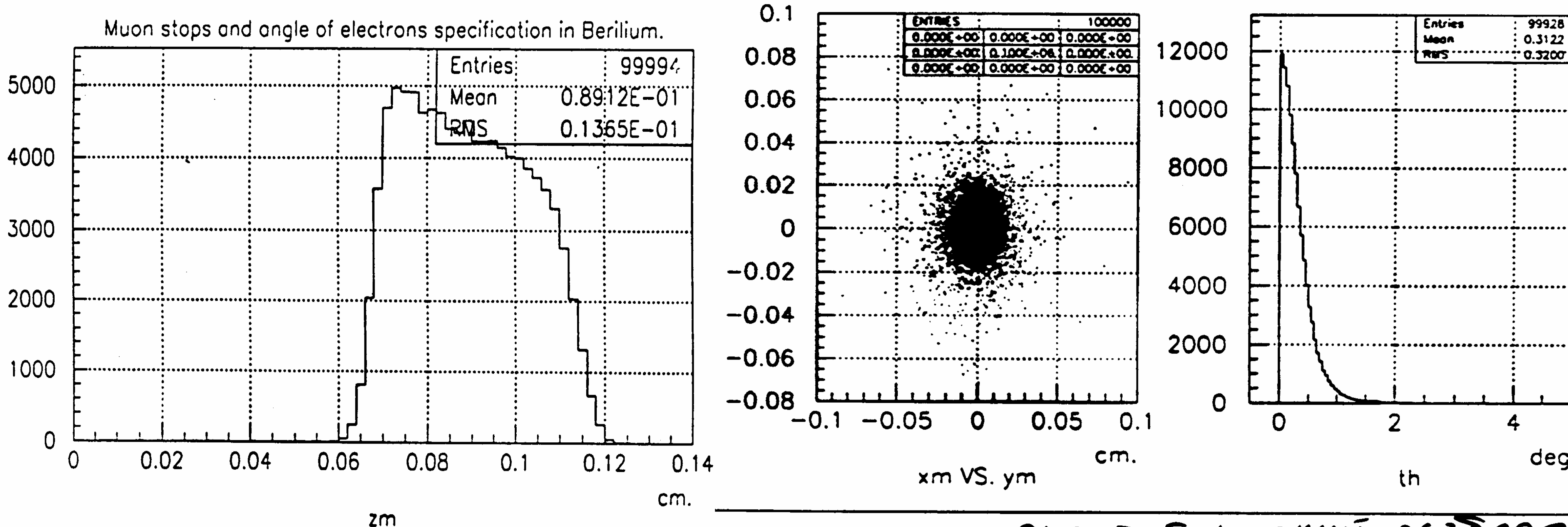

энергетический разброс
пучка после мишени

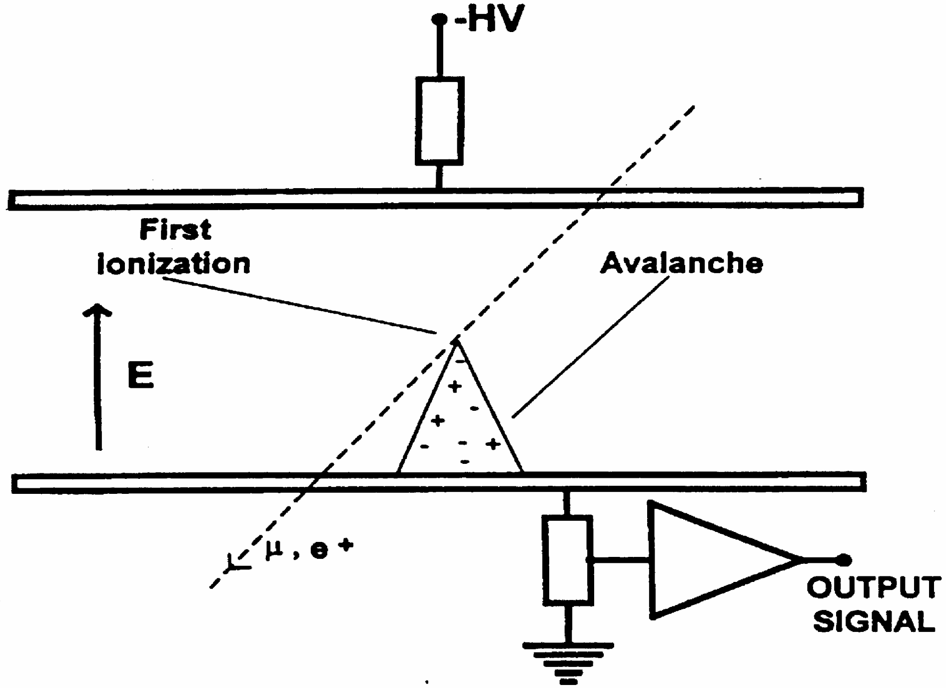

Figure 11: The Plane Parallel Chamber.

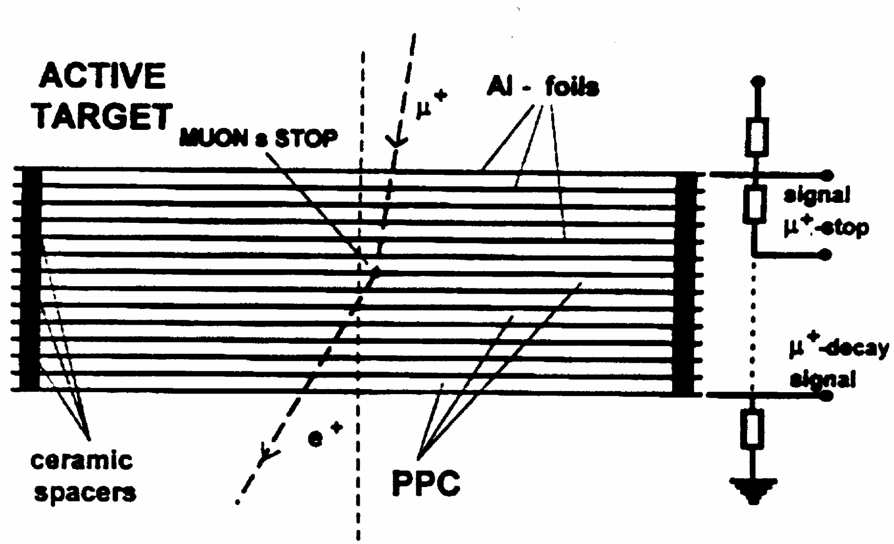

Figure 12: The Multi PPC structure as an Active target.

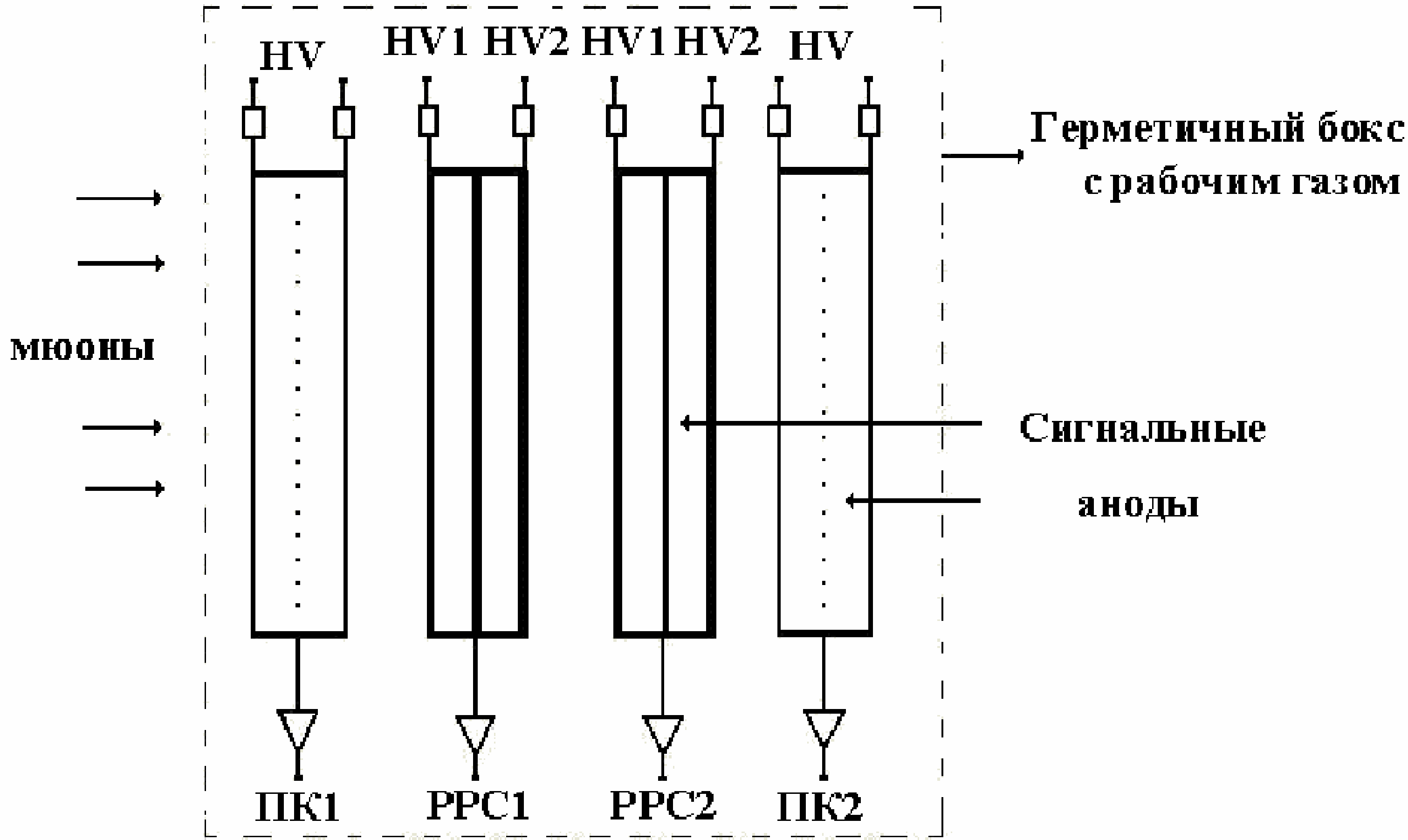
HV
HV1 HV2 HV1 HV2
HV
Герметичный бокс
с рабочим газом
мюоны
Сигнальные
аноды
ПК1
РРС1
РРС2
ПК2

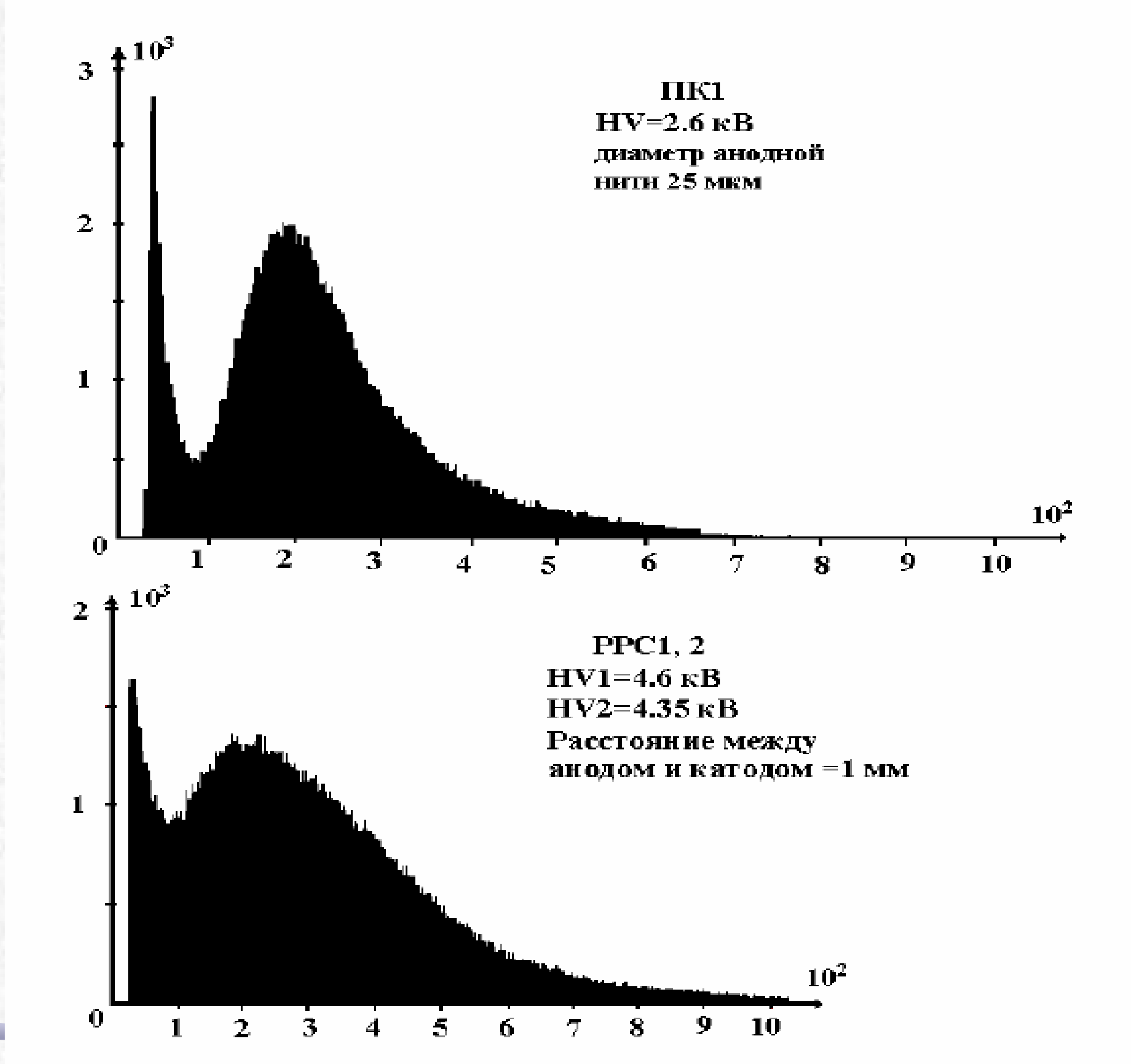

ПК1
HV=2.6 кВ
диаметр анодной
нити 25 мкм
10^3
3
2
1
0
1
2
3
4
5
6
7
8
9
10
10^2
РРС1, 2
HV1=4.6 кВ
HV2=4.35 кВ
Расстояние между
анодом и катодом =1 мм
10^3
2
1
0
1
2
3
4
5
6
7
8
9
10
10^2

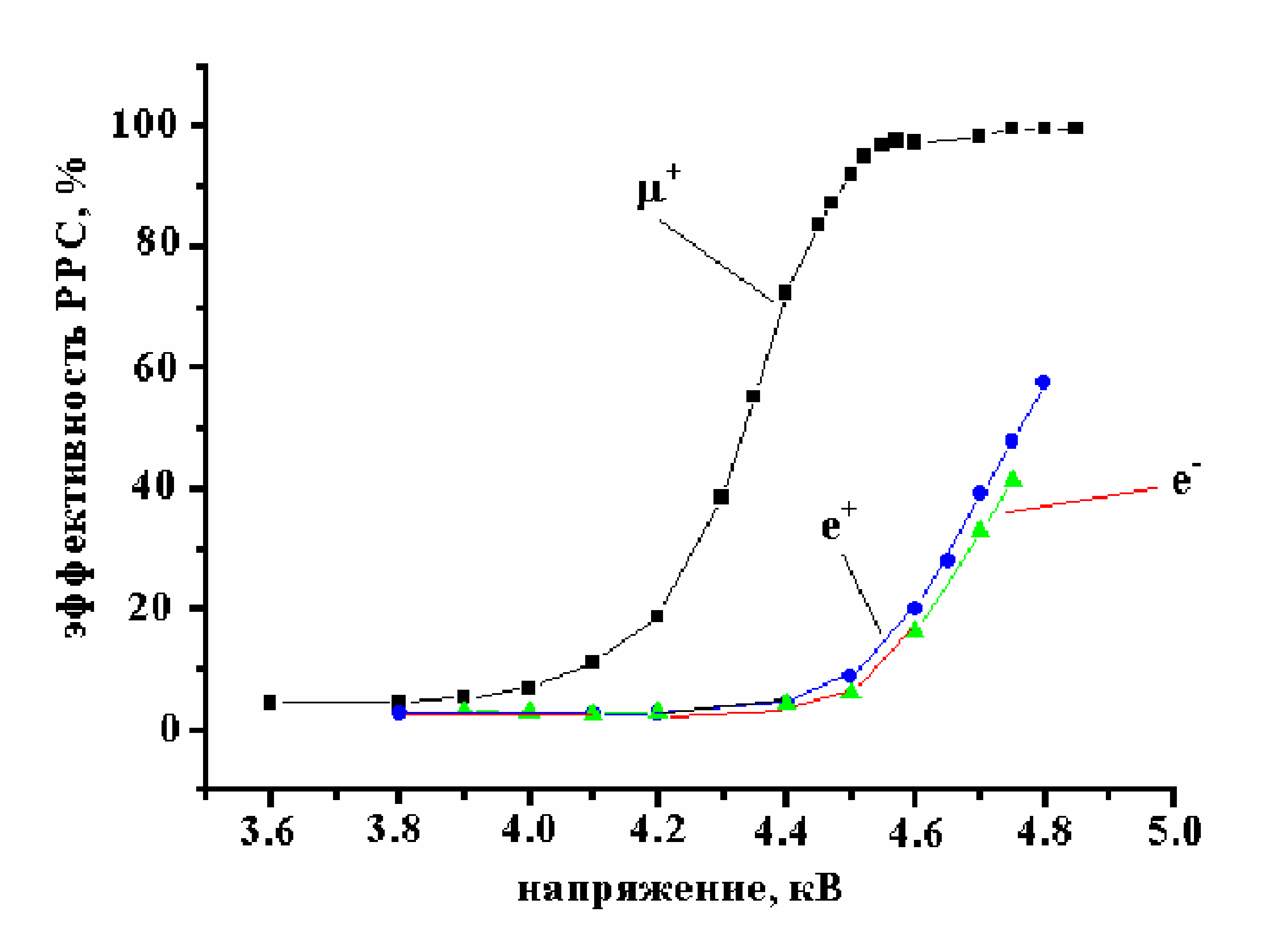

эффективность РРС, %
100
80
60
40
20
0
3.6
3.8
4.0
4.2
4.4
4.6
4.8
5.0
напряжение, кВ
μ^+
e^+
e^-

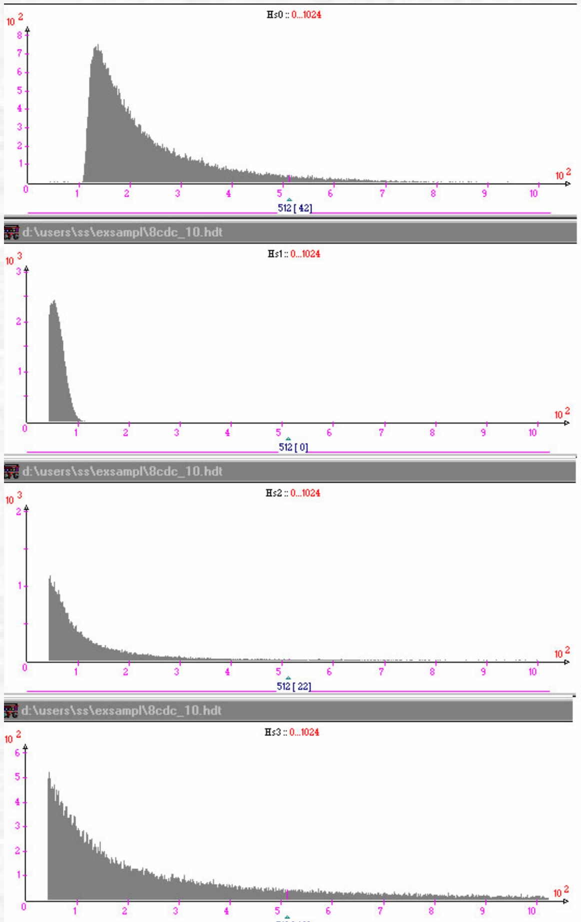
Hs0 :: 0...1024
512 [42]
d:\users\ss\exsampl\8cdc_10.hdt
Hs1 :: 0...1024
512 [0]
d:\users\ss\exsampl\8cdc_10.hdt
Hs2 :: 0...1024
512 [22]
d:\users\ss\exsampl\8cdc_10.hdt
Hs3 :: 0...1024
512 [43]

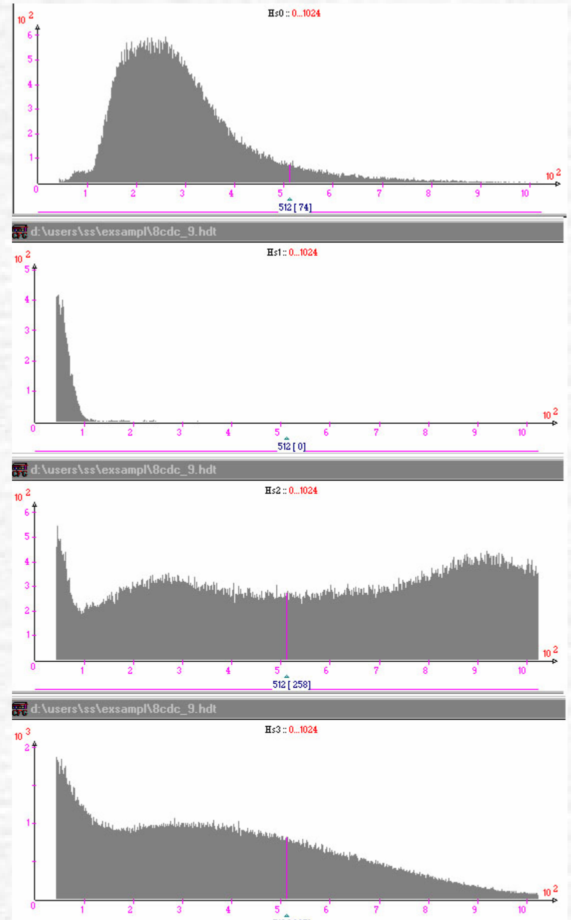
Hs0 :: 0...1024
512 [74]
d:\users\ss\exsampl\8cdc_9.hdt
Hs1 :: 0...1024
512 [0]
d:\users\ss\exsampl\8cdc_9.hdt
Hs2 :: 0...1024
512 [258]
d:\users\ss\exsampl\8cdc_9.hdt
Hs3 :: 0...1024
512 [827]

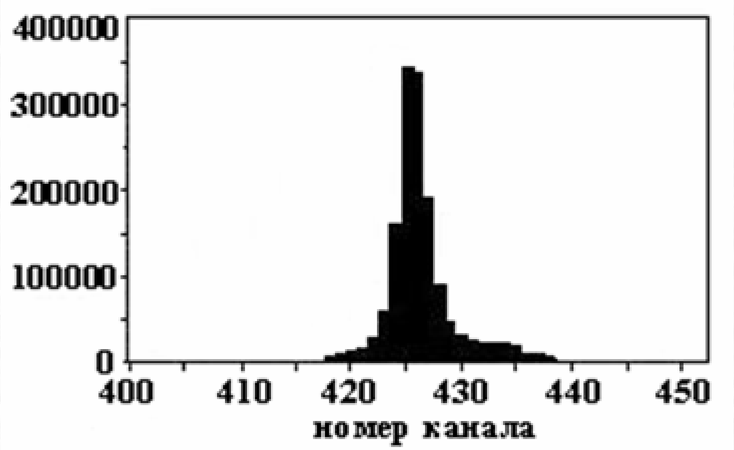

Рис. 5. Временное разрешение РРС газовым зазором 1мм (в одном канале гистограммы 0,625 нс).

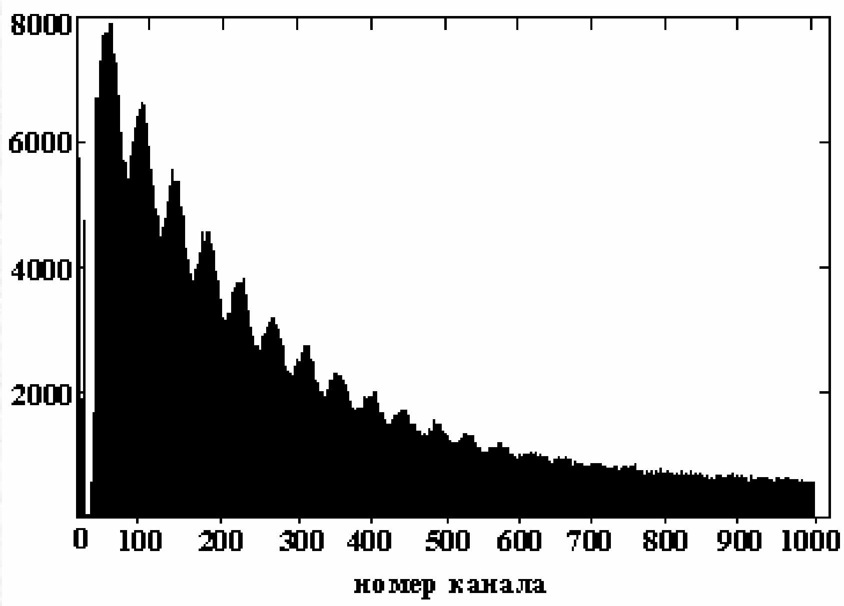

Рис. 6. SR - спектр.

Project FAMILON II

In order to improve of the TRIUMF experiment and to get $R_\alpha \leq 3.10^{-8}$, it is necessary to have the energy resolution $\Delta\varepsilon/\varepsilon \sim 10^{-4}$, the time measurement accuracy of 250 ps, the solid angle $\Omega \sim 1.2$ sr, and the rate of muon stops of 2.106 s-1. It takes approximately 1000 hours of beam time on the 99% polarized "surface" muon beam.

To realize it, we propose to create the μSR-spectrometer using the Time Projection Chamber to measure the momentum of a positron and a set of the Plane Parallel chambers as an active target to obtain the μSR-spectrum.

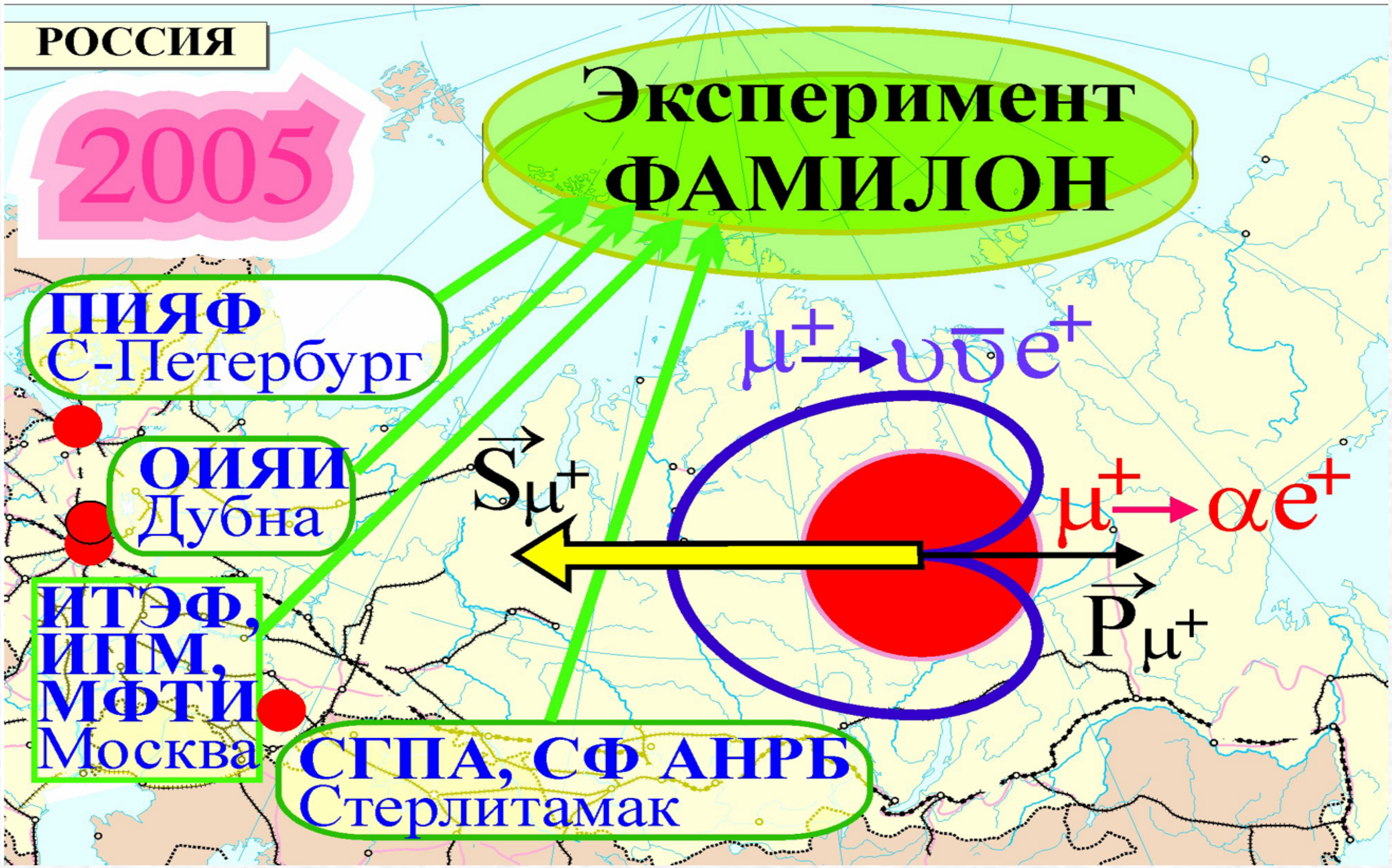
РОССИЯ
2005
Эксперимент
ФАМИЛОН
ПИЯФ
С-Петербург
ОИЯИ
Дубна
ИТЭФ,
ИПМ,
МФТИ
Москва
СГПА, СФ АНРБ
Стерлитамак
$\mu^+ \rightarrow \upsilon\bar{\upsilon}e^+$
$\vec{S}_{\mu^+}$
$\mu^+ \rightarrow \alpha e^+$
$\vec{P}_{\mu^+}$

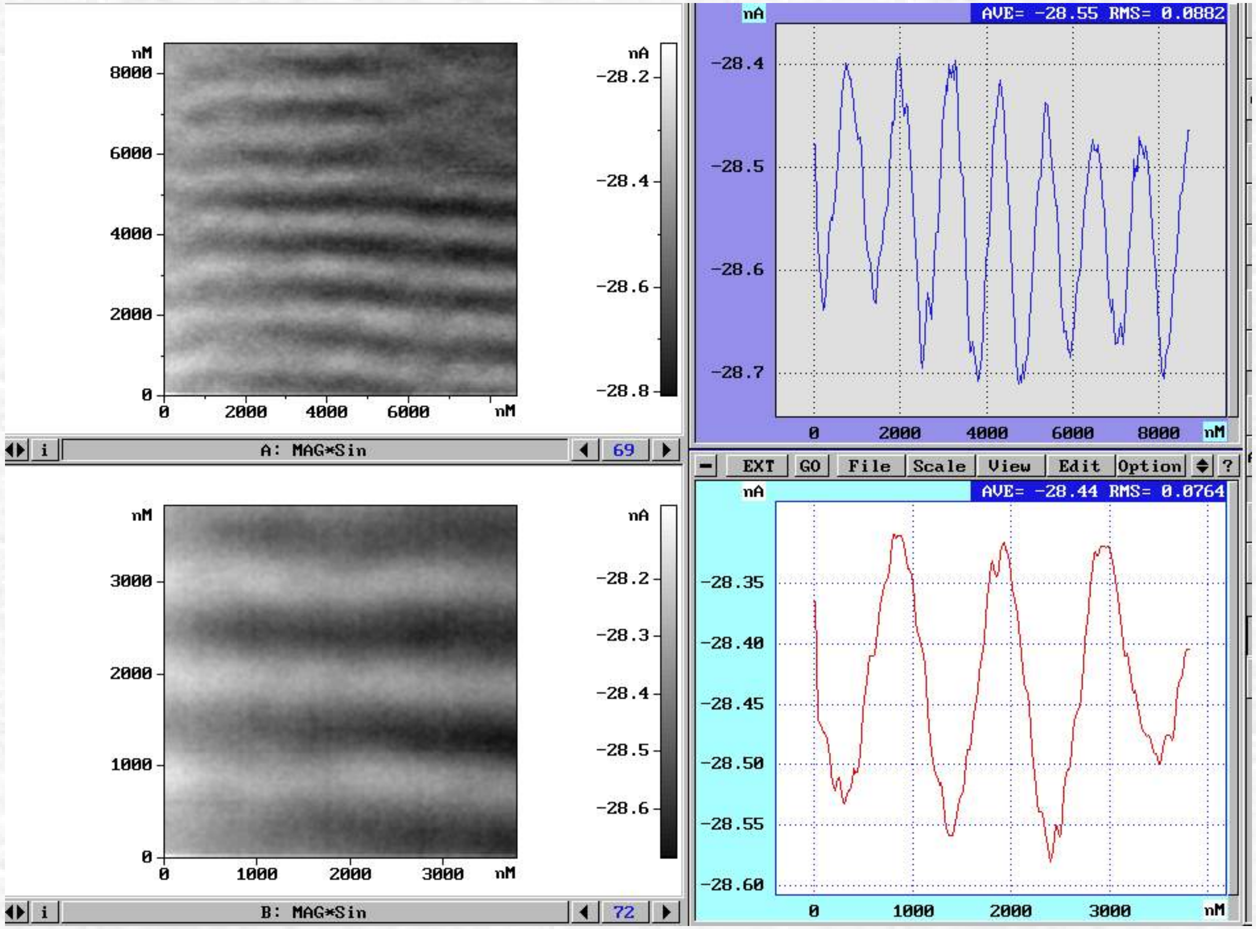

Фазовые контрасты МСМ режима поверхности исходной трансформаторной стали. Профилограммы вдоль оси Y при X = 4 мкм и X = 2 мкм соответствующих сканов

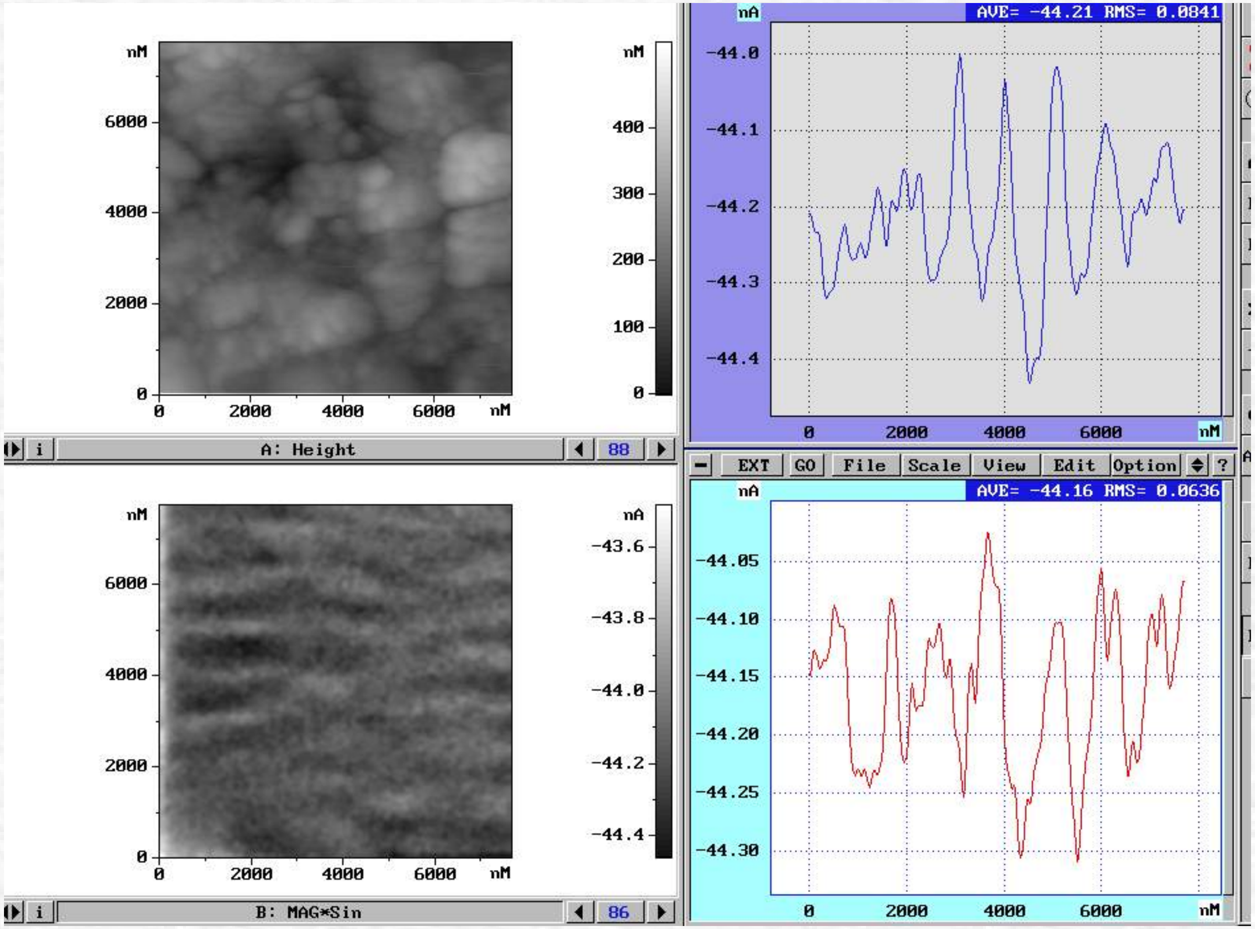

Топография и фазовый контраст МСМ режима поверхности намагниченной трансформаторной стали. Профилограммы фазового контрасты выполнены вдоль оси Y при X = 2 мкм (верхняя) и X = 4 мкм (нижняя)

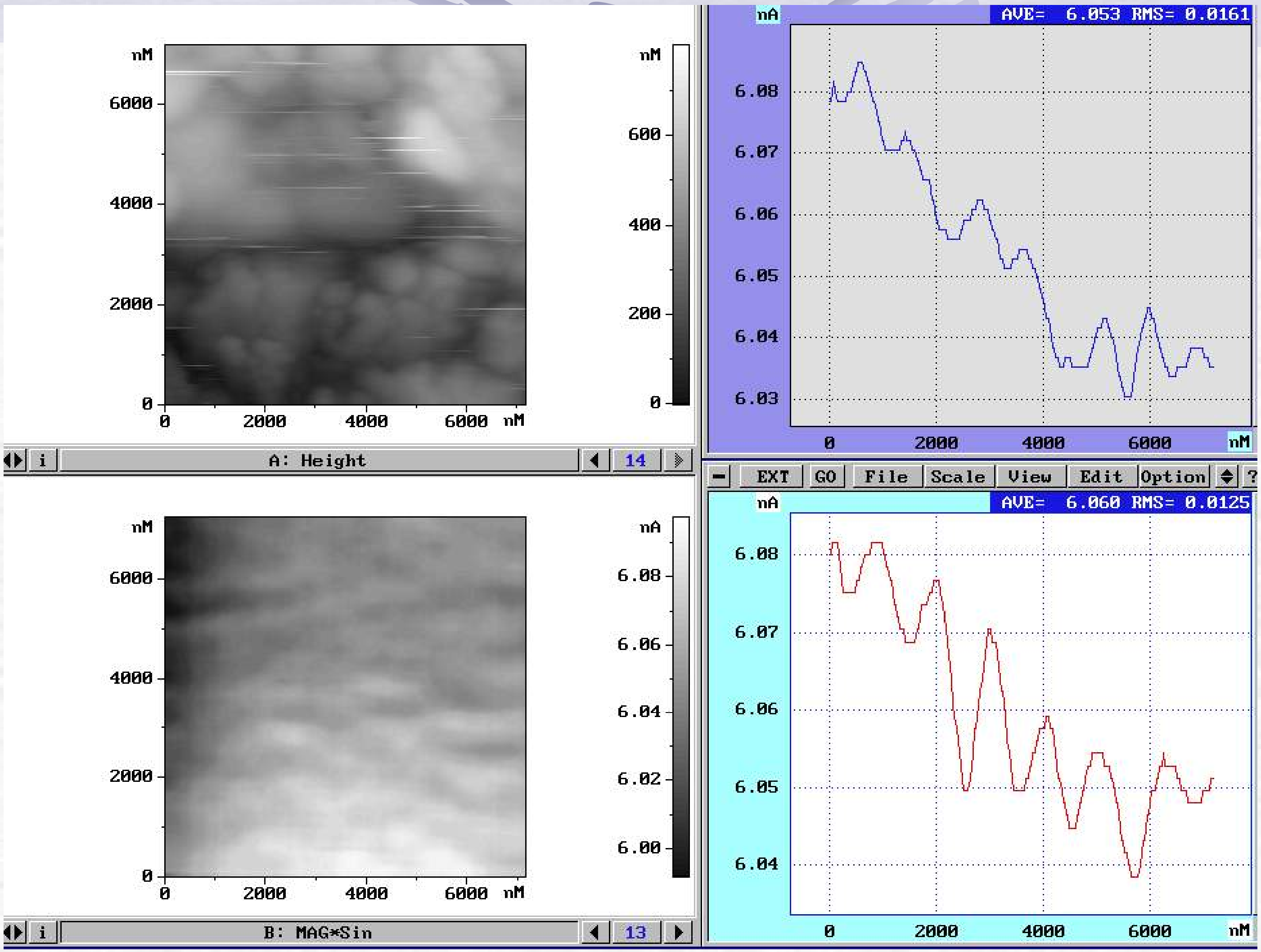

Топография и фазовый контраст МСМ режима поверхности отожжённой трансформаторной стали. Профилограммы фазового контрасты выполнены вдоль оси Y при X = 2 мкм (верхняя) и X = 6,5 мкм (нижняя)

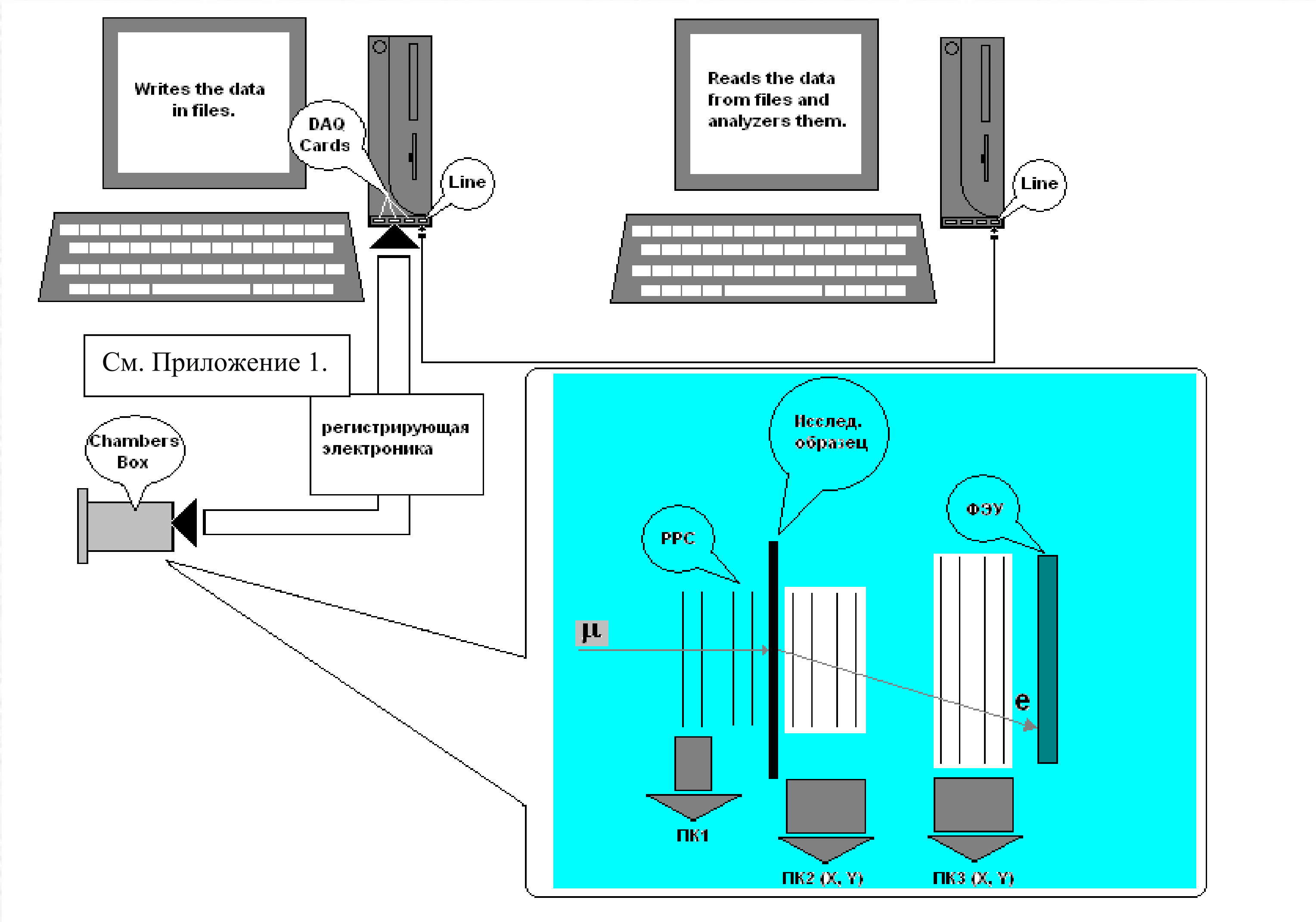

Рис.1. Схема постановки эксперимента.

Блок-схема регистрирующей электроники детектора.

СЦ- сцинтиллятор;
ПК1-ПК3 – пропорциональные камеры;
РРС- плоскопараллельная камера;
ФЭУ1-ФЭУ2- фотоэлектронные умножители;
ПУ- предусилитель;
4ФК- формирователь с компенсацией амплитудного влияния;
Ф- формирователь;
Д- дискриминатор;
ПВК- преобразователь время-код.

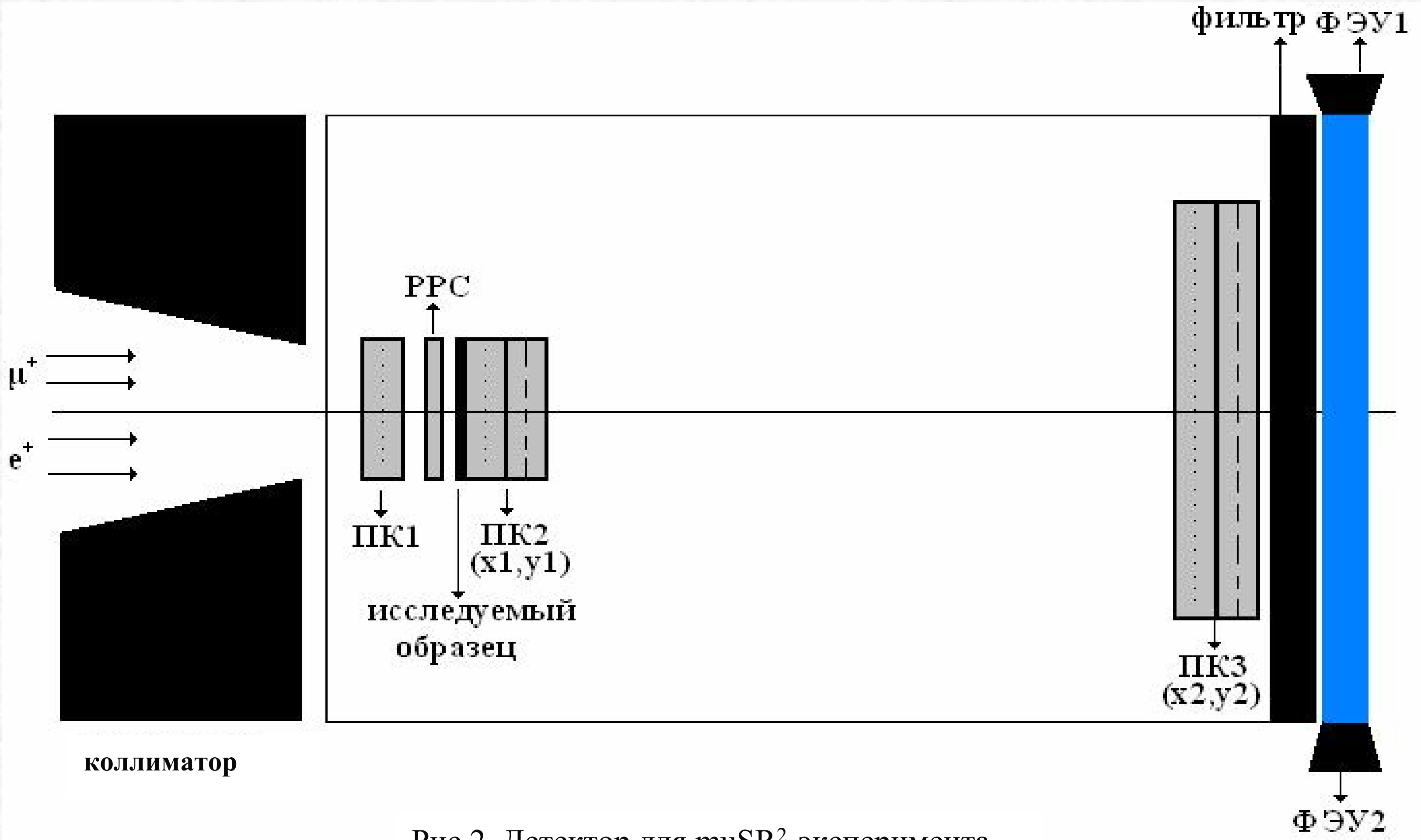

Рис.2. Детектор для muSR²-эксперимента.

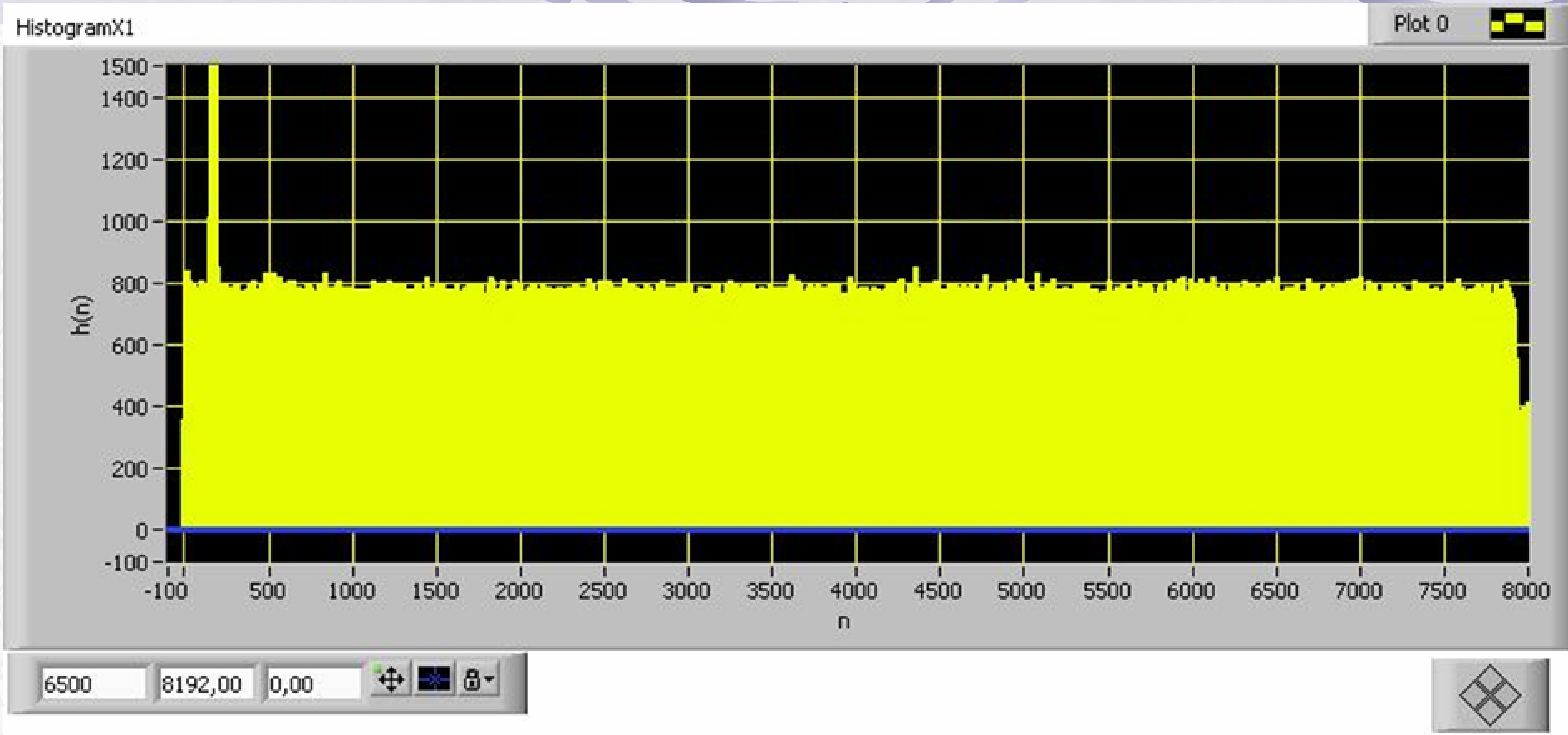

Рис. 8. Работа TDC (то же самое, что и рис. 7).

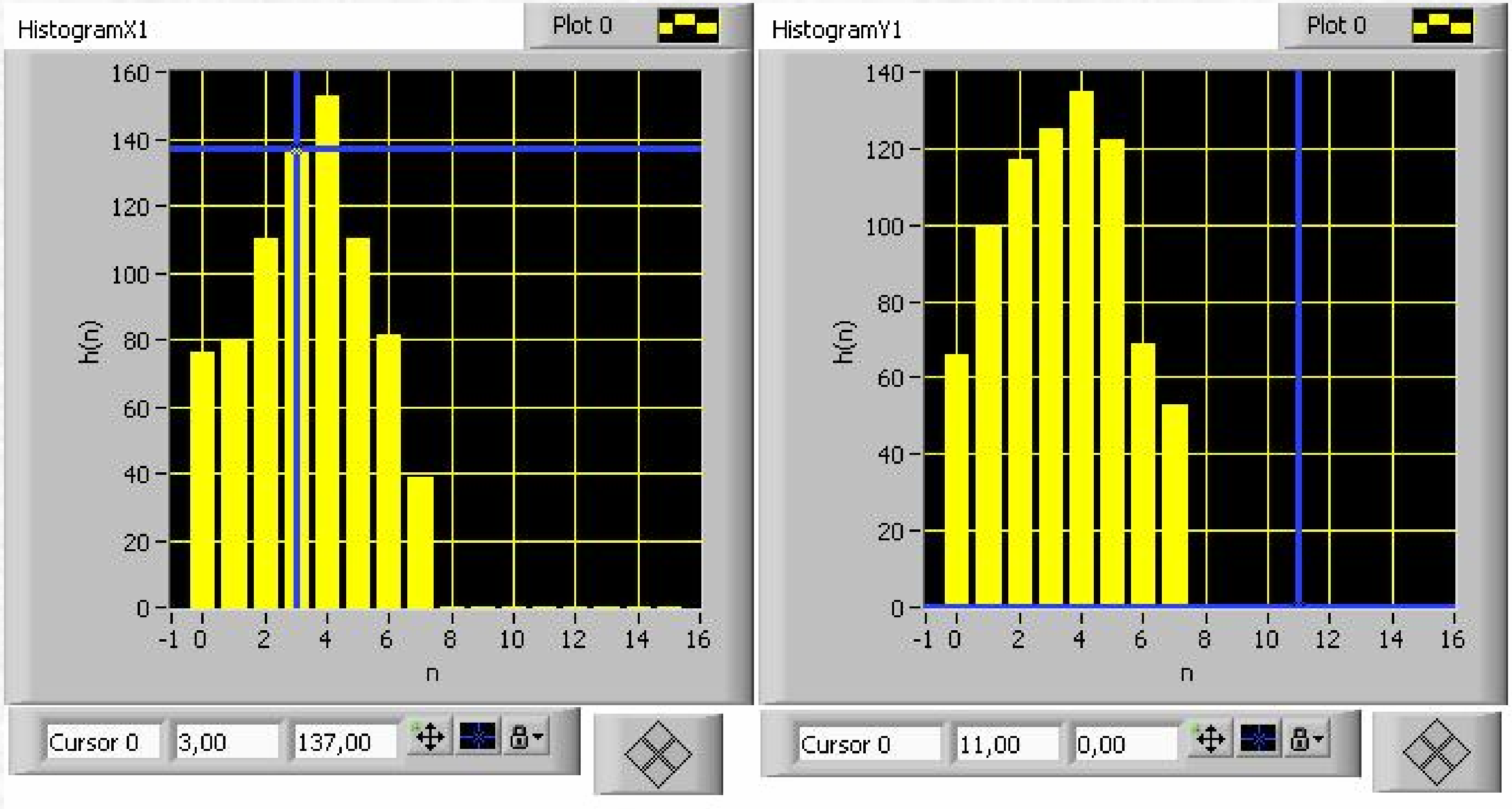

Рис. 10. Координатная система ПК2 (X1, Y1).

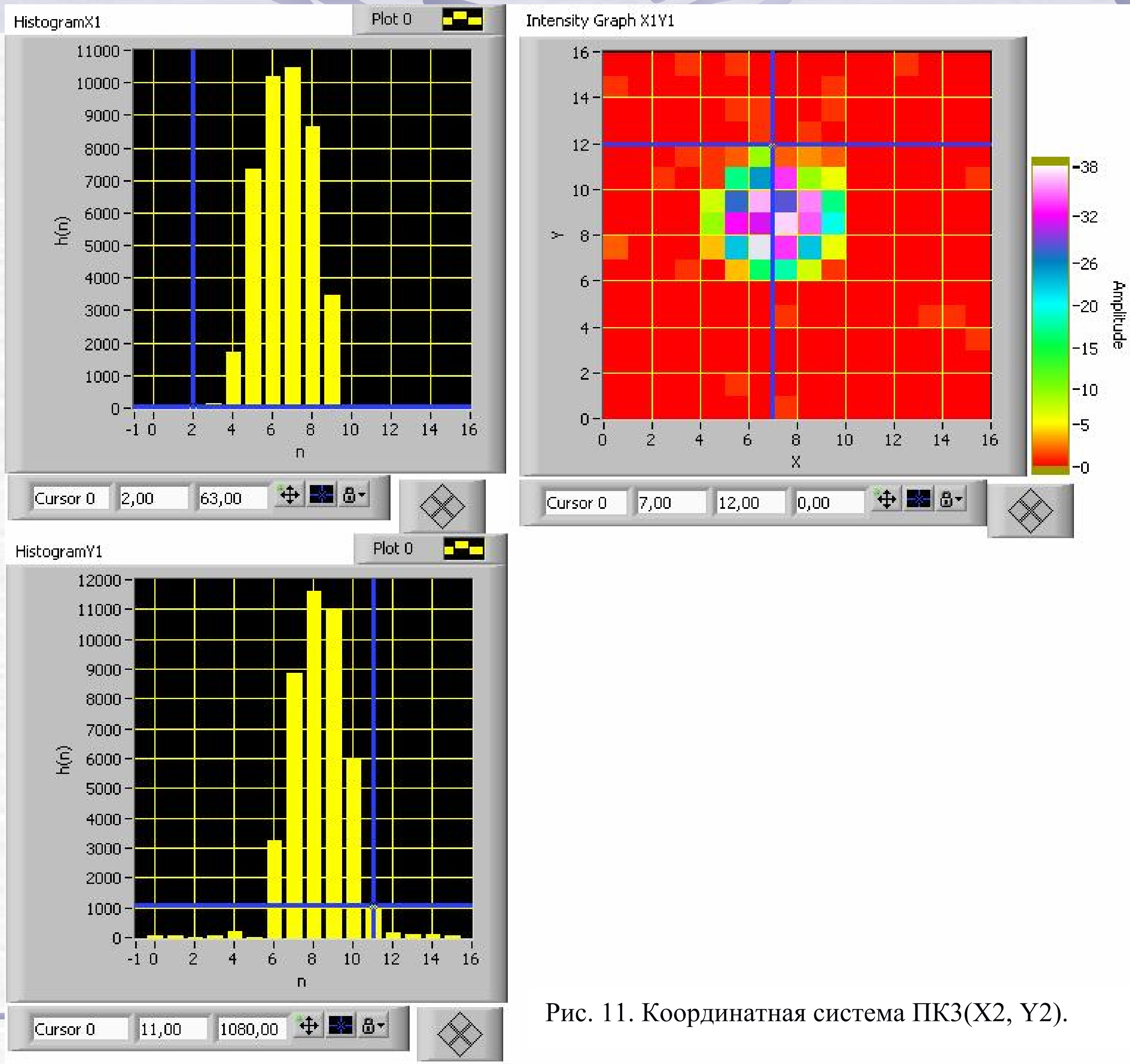

Рис. 11. Координатная система ПК3(X2, Y2).

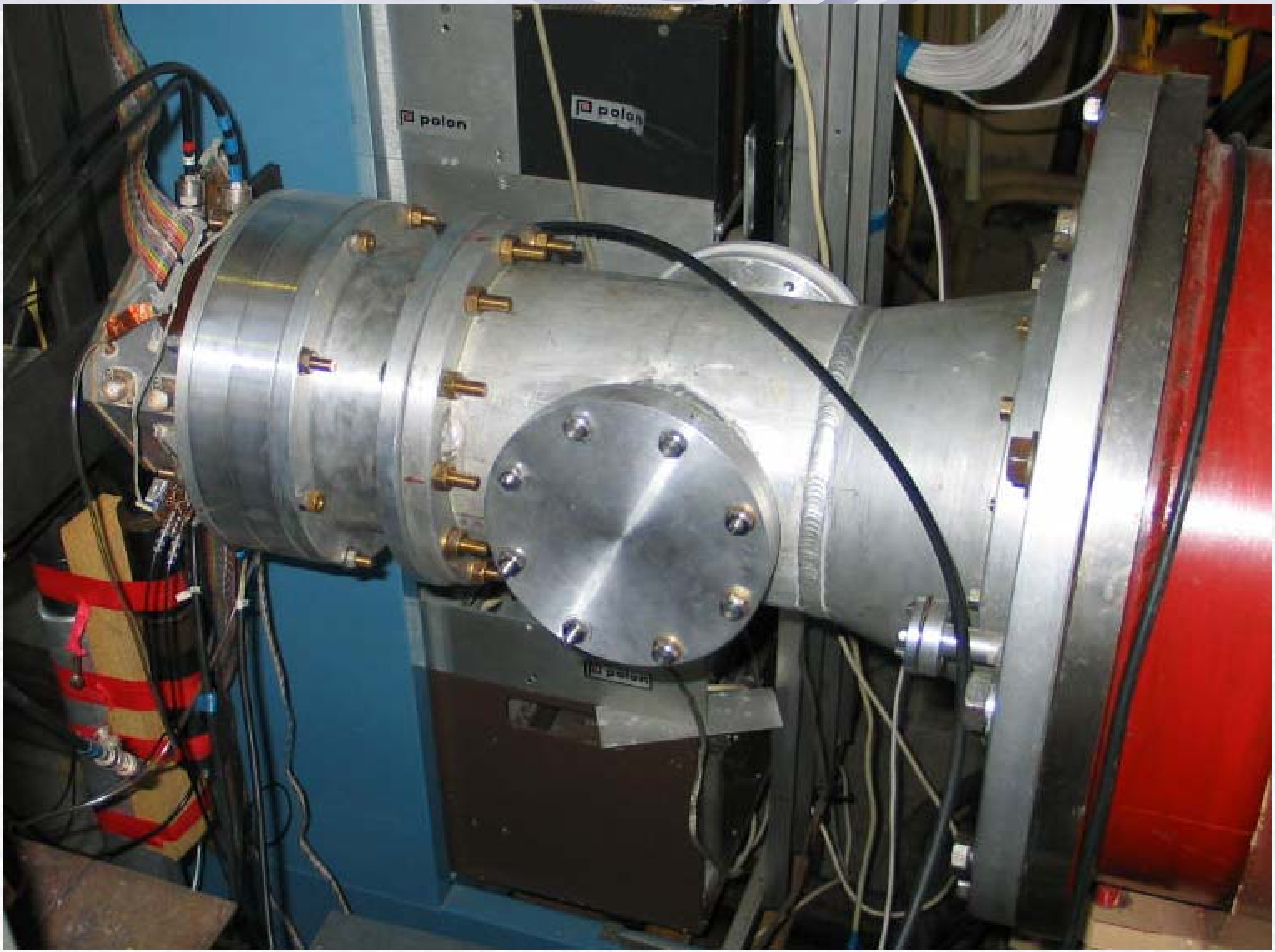
polon
polon
polon